

A journey from solution self-assembly to designed interfacial assembly

Edwin C. Constable¹

Department of Chemistry, University of Basel, Basel, Switzerland

¹ Corresponding author: e-mail address: edwin.constable@unibas.ch

Contents

1. Introduction
2. From coordination chemistry to metallosupramolecular chemistry
 - 2.1 Coordination chemistry as molecular recognition
 - 2.2 Metal-binding domains
 - 2.3 Metallosupramolecular chemistry
 - 2.3.1 Partitioning metal-binding domains in polydentate ligands
 - 2.3.2 Symmetrical partitioning of metal-binding domains in helical metallosupramolecules
 - 2.3.3 Asymmetrical partitioning of metal-binding domains in helical metallosupramolecules
 - 2.4 From pure compounds to libraries

- 3.** Supramolecular chemistry at surfaces
 - 3.1** Overview of supramolecular interactions
 - 3.2** Self-assembly at surfaces
 - 3.3** Combining self-assembly and metallosupramolecular chemistry at surfaces
 - 3.4** From self assembly to covalent attachment
 - 3.4.1** Surface and anchoring algorithms – the new toolkit
 - 3.5** Taking metallosupramolecular chemistry to surfaces
 - 3.5.1** The dye-sensitized solar cell (DSC)
 - 3.5.2** Copper DSCs
 - 3.6** From "complexes as metals/complexes as ligands" to "surfaces as ligands, surfaces as complexes"
 - 3.6.1** Sequential assembly of copper DSCs – the library of anchors
 - 3.6.2** Sequential assembly of copper DSCs – the library of ancillary ligands
 - 3.6.3** Atom economy and regeneration
 - 3.6.4** The future
- 4.** Acknowledgements
- 5.** References

Abstract

This article describes the development of concepts in metallosupramolecular chemistry. In particular, the transfer of the concepts from solution phase to metallosupramolecular chemistry at solid-fluid interfaces is discussed. The concept of metal-binding domains is quantified and used for the design of ligands for specific supramolecular applications. The use of weak interactions for the investigation of surface supramolecular chemistry is presented followed by the "surfaces as ligands, surfaces as complexes" approach for the design of functional devices. This conceptual development is placed in the context of the author's own laboratory.

1. INTRODUCTION

Self-assembly and self-organization are paradigms that have become intimately and irrevocably associated with supramolecular chemistry in its transition from chemical novelty to established discipline and methodology. Nevertheless, the terms are frequently used loosely and interchangeably, and it is appropriate to clarify what we understand by each in the context of this article and in the broader context of supramolecular chemistry.

The definition of supramolecular chemistry itself is not simple, but the formulation “... *supramolecular chemistry concerns the mutual interaction of molecules or molecular entities with discrete properties. This interaction is usually of a noncovalent type (an “intermolecular bond” such as a hydrogen bond, dipolar interaction, or π -stacking)*” finds wide acceptance (1). For this article, we will extend the definition to include interactions of this nature between partners in which one of the entities is an extended structure which does not necessarily have discrete properties. Philosophical discussions regarding the difference between self-assembly and self-organization are prevalent in the literature, with view-points ranging from the agnostic to those of ardent crusaders. A useful and widely accepted differentiation is to distinguish “self-organization from self-assembly on a thermodynamic basis, where self-organization implies a non-equilibrium process and self-assembly is reserved for spontaneous processes tending toward equilibrium” (2). The definitions become blurred in the context of interfacial processes, in which the convention is to set the activity of a pure solid to a numerical value of one.

This account is about a journey from “traditional” coordination chemistry, through solution phase supramolecular chemistry to the use of the paradigms and methodologies of self-organization and self-assembly in the construction of ordered and hierarchical structures at solid-fluid interfaces. At the end phase of this journey, interactions with atomically well-defined and low-dimensional surfaces as well-as complex nanostructured surfaces will be considered.

2. FROM COORDINATION CHEMISTRY TO METALLOSUPRAMOLECULAR CHEMISTRY

2.1 Coordination chemistry as molecular recognition

“What goes around comes around” - this journey begins with the design of 2,2'-bipyridine ligands for application in what came to be known as dye-sensitized solar cells and ends in the development of new methodologies for the design of these and related systems. Rutile (TiO_2) is a semiconductor with a band gap of ≈ 3.0 eV and exhibits no photocurrent upon irradiation with light $\lambda > 450$ nm. In contrast, the complex $[\text{Ru}(\text{bpy})_2(\mathbf{1})]$ exhibits a typical $\{\text{Ru}^{\text{II}}(\text{bpy})_3\}$ absorption close to 450 nm. The complex $[\text{Ru}(\text{bpy})_2(\mathbf{1})]$ binds to the surface of single crystal rutile and acts as a photosensitizer, allowing the photoinjection of electrons directly into the conduction band upon irradiation with visible light $\lambda > 450$ nm (Figure 1) (3). The photocurrents were modest and it was only when Grätzel used this strategy for the modification of nanostructured TiO_2 surfaces, allowing very high dye-loading, that the method became viable (4,5,6).

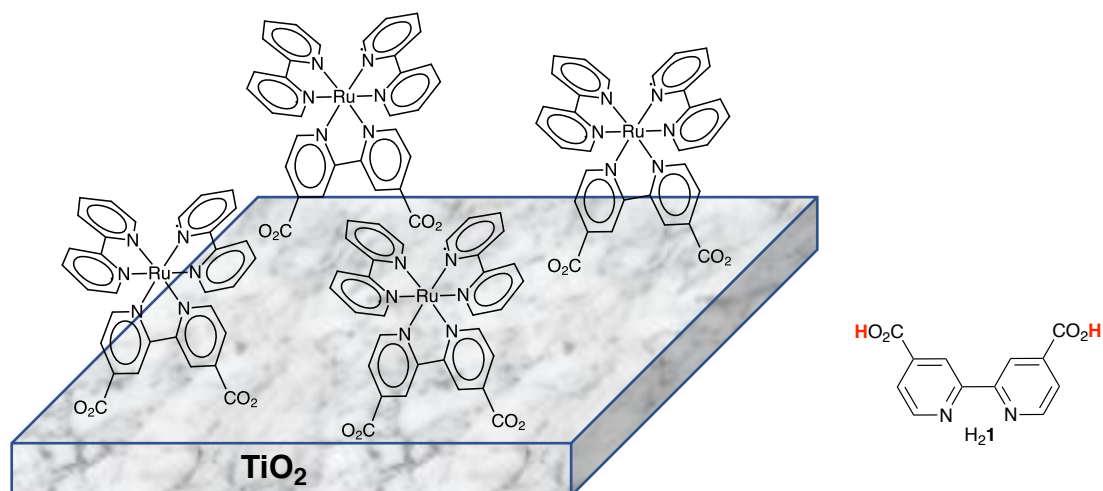


Figure 1 Schematic representation of $[\text{Ru}(\text{bpy})_2(\mathbf{1})]$ molecules on a TiO_2 surface and the structure of ligand $\text{H}_2\mathbf{1}$.

These studies of 2,2'-bipyridine chemistry resulted in two observations which define the direction of the research reported in this chapter. The first observation was that novel coordination chemistry was predicated upon the ability to design and synthesize bespoke ligands which incorporated specific functionality and which would impart desired properties into their complexes. The second was an observation that although complexes of 2,2'-bipyridines (7,8) and 1,10-phenanthrolines (9) had been widely studied, at the beginning of the 1980's 2,2':6',2''-terpyridines (10,11) were exotic species and the coordination chemistry of the higher oligopyridines was virtually unexplored (10,12). In the intervening years, the chemistry of these ligands, in particular 2,2':6',2''-terpyridines, has expanded exponentially (11,13,14).

At the same time, molecular recognition was emerging as a powerful concept in organic and biomolecular chemistry (15,16). The link with coordination chemistry

was made with the award of the 1987 Nobel Prize for Chemistry to Cram, Lehn and Pedersen "for their development and use of molecules with structure-specific interactions of high selectivity" (17). In his Nobel lecture, Lehn talks extensively of molecular recognition and makes a direct link to the specificity of the binding of group 1 and group 2 metal ions by crown ethers and cryptands of various sizes (18). Although the initial association of coordination chemistry with molecular recognition was based upon the size of the metal ion, it was only a matter of time before the concepts familiar to inorganic chemists would be combined to emerge as the new field of metallocsupramolecular chemistry.

It should be noted that in the 1970's and early 1980's, coordination chemistry was regarded as old-fashioned and a poor-relation of the "new" organometallic chemistry. Concepts for ligand design were often naïve, although a good understanding of thermodynamic concepts such as the chelate (19,20,21,22) and macrocyclic effects (23) together with the principle of hard and soft acids and bases proved to be powerful tools (24). Also important was the knowledge of the enormous kinetic variation between "labile" and "inert" metal centres (25)

2.2 Metal-binding domains

The oligopyridines will play a central role in this story and it is appropriate to present their structures and the abbreviations that will be used (Fig. 2). We developed the concept of metal-binding domains to assist us in the design of polytopic ligands. The ligand **2** is a 6,6'-functionalized 2,2'-bipyridine which also has two additional nitrogen atoms which could coordinate to a metal ion. In this trivial case, we easily identify the

bpy metal-binding domain. Similarly, the ligand **3** contains a readily identified tpy metal-binding domain together with two additional potential donor atoms.

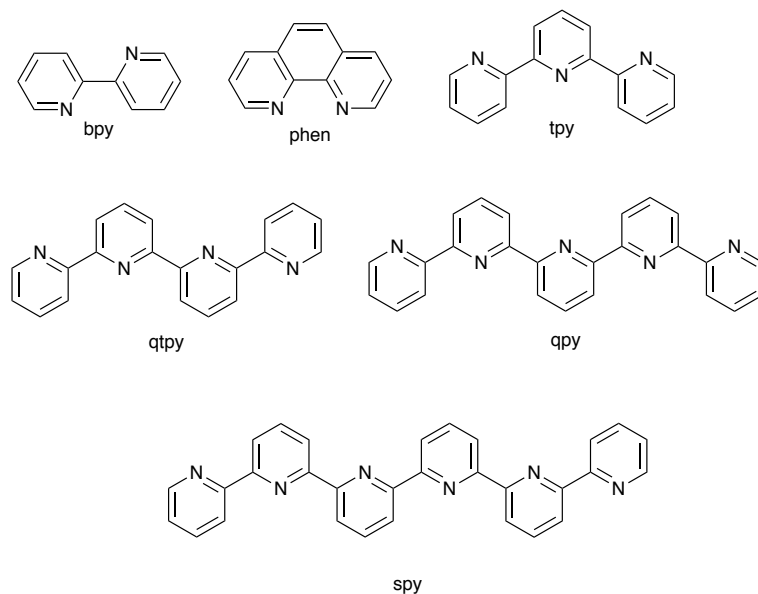


Figure 2 Typical nitrogen donor ligands and metal-binding domains 2,2'-bipyridine (bpy), 1,10-phenanthroline (phen), 2,2':6',2''-terpyridine (tpy), 2,2':6',2'':6'',2'''-quaterpyridine (qtpy), 2,2':6',2'':6'',2''':6''',2''''-quinquepyridine (qpy) and 2,2':6',2'':6'',2''':6''',2''''-sexipyridine (spy).

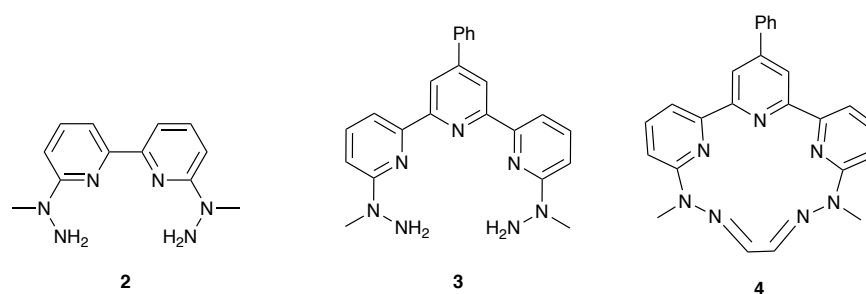
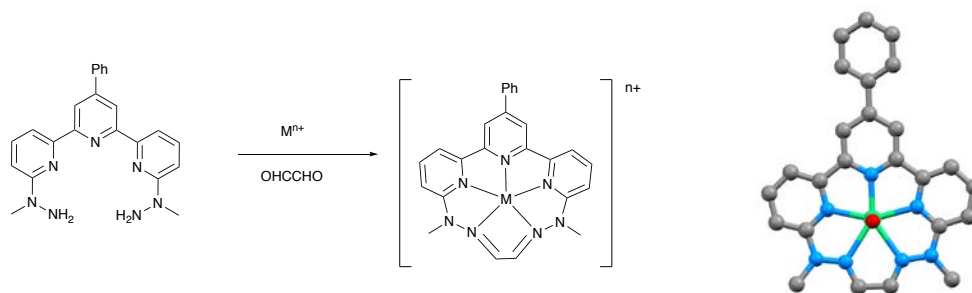


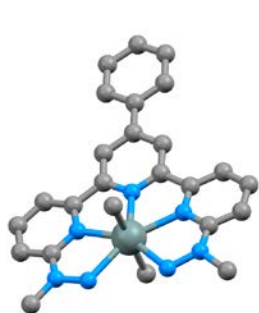
Figure 3 Hydrazino-functionalized ligands **2** and **3** which contain bpy and tpy metal-binding domains respectively. Also shown is the macrocycle **4** which contains a tpy metal-binding domain.



Scheme 1 The template reaction of the bis(hydrazine) **3** with glyoxal in the presence of a metal ion to give a complex of the macrocycle **4** containing a tpy metal-binding domain. The solid state structure of the cation $[\text{Ni}(\mathbf{4})(\text{EtOH})_2]^{2+}$ looking along the O-Ni-O vector is also shown (hydrogen atoms and the carbon atoms of the axial ethanol ligands have been omitted for clarity).

Compound **3** was initially prepared to investigate metal-ion templated synthesis of the macrocycle **4**, but in the course of those studies some unexpected results gave insight into the subtlety of metal-ligand recognition events and prompted additional investigations leading to the further development of metallosupramolecular chemistry. Ligand **4** was in part designed out of perversity – five coordinate complexes in general were relatively uncommon and complexes with planar pentadentate ligands were extremely rare. The design of **4** was predicated on the use of the tpy metal-binding domain to stabilize d-block metal complexes of both **3** and **4**, which, in turn, would facilitate the desired template reaction with glyoxal (Scheme 1). Nickel(II) salts proved to be effective template ions giving the pentagonal bipyramidal complex $[\text{Ni}(\mathbf{4})(\text{EtOH})_2]^{2+}$ in good yield (26,27). Frustratingly, no other first row transition metal ion proved to be effective for the template condensation. For reasons which are

lost in the mists of time, we investigated the use of Me_2SnCl_2 as a template; the pentagonal bipyramidal cation $[\text{Me}_2\text{Sn}(\mathbf{3})]^{2+}$ (**28**) was readily prepared by the direct reaction of Me_2SnCl_2 with **3** (Figure 4a) but upon cyclization with glyoxal, the product was the metal-free species $\text{H}_2\mathbf{4}^{2+}$ (Figure 4b) (**27**). A detailed analysis of the structural data for $[\text{Me}_2\text{Sn}(\mathbf{3})]^{2+}$ and $\text{H}_2\mathbf{4}^{2+}$ revealed that the cyclization reduces the size of the bonding cavity, most readily seen in the reduction of the distance between the amino nitrogens in **3** of 3.222 Å to 2.641 Å in $\text{H}_2\mathbf{4}^{2+}$. As a consequence the cavity is too small for the Me_2Sn moiety and the presence of the two axial methyl groups prevents the typical response of moving the metal out of the plane of the ligand – this was the first of a number of examples of what we termed the transient template effect (**27,29,30**). The result is the labilization of the entire Me_2Sn unit and the isolation of the free macrocycle. Observations of this nature indicated to us that a better understanding of the molecular recognition processes involving metal ions could result in novel and exciting chemistry.



(a)



(b)

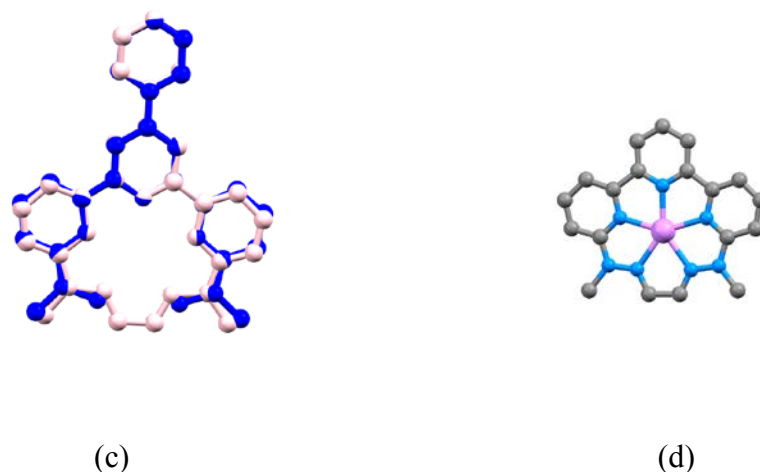


Figure 4 The solid state structures of the complexes a) $[\text{Me}_2\text{Sn}(\mathbf{3})]^{2+}$ b) $\text{H}_2\mathbf{4}^{2+}$ where the two acid protons lie within the N_5 cavity c) an overlay of the core in these two compounds, showing the origin of the transient template effect lies in the reduction in the binding cavity associated with the terminal nitrogen atoms of the hydrazine moving closer in the macrocycle and d) the lithium complex of an analogue of **4**. Hydrogen atoms have been omitted for clarity.

Inspection of compounds **3** and **4** highlighted the similarity of the donor set to that in qpy (Figure 5); in each case five potential donor nitrogen atoms are separated by two fully conjugated nitrogen or carbon backbone atoms. In retrospect, this analogy proved to be rather naïve but it allows us to develop the themes of metal-binding domains further within the framework of metallocsupramolecular chemistry. Nevertheless, the supposed similarity between qpy and **4** lead to some interesting observations. One of the very few compounds reported for qpy was the species $\text{Li}(\text{ClO}_4)\cdot\text{qpy}$ (31) and more in the spirit of hope than expectation we reacted $[\text{H}_2\mathbf{4}][\text{PF}_6]_2$ with LiOH and were surprised to obtain the remarkably stable complex $[\text{Li}(\mathbf{4})][\text{PF}_6]$ which may be recovered unchanged from boiling water (Figure 4c

illustrates an analogue which does not possess the 4'-phenyl substituent on the tpy) (32). The lithium ion is in a planar pentadentate coordination environment and ^7Li NMR spectroscopic studies revealed no exchange between the coordinated lithium and bulk lithium chloride solution.

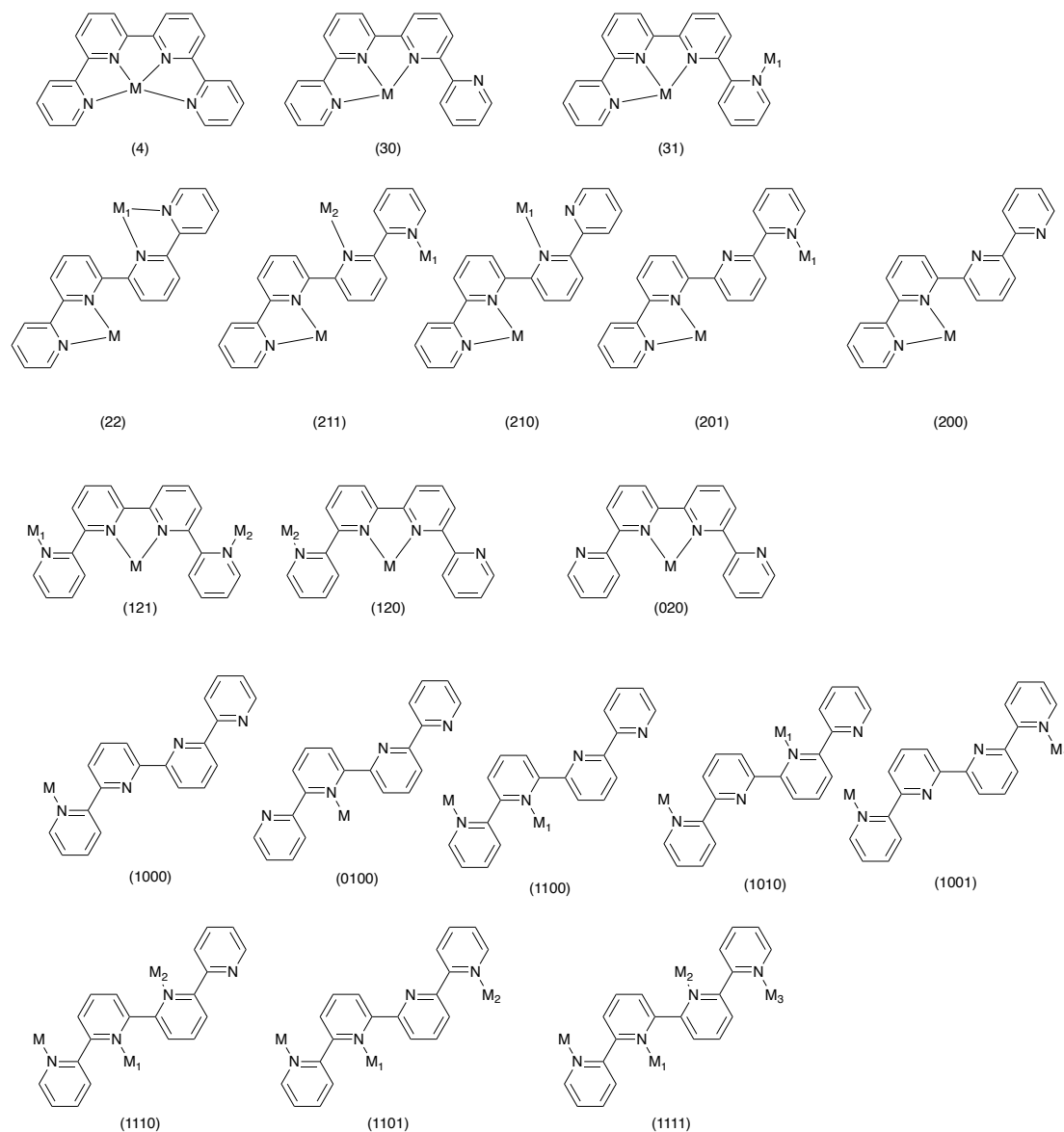


Figure 5 The possible bonding modes of a qtpy ligand. Modes in which a nitrogen donor bonds to two metal centres are omitted as they are a degenerate representation of the modes above. The nomenclature system is discussed in detail in Section 2.3.1. The metal centres M, M_1 , M_2 and M_3 may be the same or different.

2.3 Metallosupramolecular chemistry

The term metallosupramolecular chemistry was introduced to try to distinguish supramolecular interactions involving or predicated upon metal-ligand interactions from those involving more conventional weak interactions (33). It does not seem fruitful to enter into discussions as to whether metal-ligand interactions are “intermolecular bonds”. Metallosupramolecular chemistry is concerned with identifying the molecular recognition features encoded in metal centres and in ligands with a view to understanding the assembly algorithms which dictate the outcome of the metal-ligand interaction. The key recognition features relating to a metal centre include the coordination number and coordination geometry, the preference for a particular type of donor atom and the spatial arrangement of the available coordination sites. The recognition features of a ligand include the number, type and spatial arrangement of the donor atoms. A second level of properties can be identified with metal centres, including oxidation state, kinetic lability or inertness, and modification of the number of available coordination sites through chelating ancillary ligands.

Combined with the idea of metal-binding domains we have now developed a powerful conceptual tool for the design of metallosupramolecules. Consider the complex *cis*-[Ru(bpy)₂Cl₂] (34); ruthenium(II) is a kinetically inert metal centre with a d⁶ electronic configuration and a very strong preference for octahedral coordination. In the case of *cis*-[Ru(bpy)₂Cl₂], four of the coordination sites are occupied by two chelating bpy ligands and so the only sites available for further coordination are

those occupied by the (more) labile chlorido ligands. A trivial example is the matching of the metal component, *cis*-[Ru(bpy)₂Cl₂], with a ligand such as phen which presents two donor atoms which complement the two labile *cis*-chlorido ligands to give [Ru(bpy)₂(phen)]²⁺ (35). A far more interesting example comes in the reaction of *cis*-[Ru(bpy)₂Cl₂] with tpy. Only two coordination sites are available at the ruthenium centre and ruthenium(II) is most unlikely to form seven-coordinate complexes, so how is the recognition mismatch between two available sites and three potential donors to be solved? The answer is both banal and paradigm breaking. The assumption of most classical coordination chemists was that a multidentate ligand such as tpy would act as a chelating tridentate ligand. In this case, the tpy ligand presents not a tridentate “tpy” metal-binding domain but a “bpy” bidentate metal-binding domain and the complex [Ru(bpy)₂(tpy-20)]²⁺ containing a bidentate tpy ligand is obtained (Figure 6) (36,37). The notation tpy-20 is described in Section 2.3.1. We described this bonding mode as hypodentate and the nomenclature is extended to include coordinated ligands in which the maximum number of potential donor atoms are not involved in binding to a metal centre (38,39).

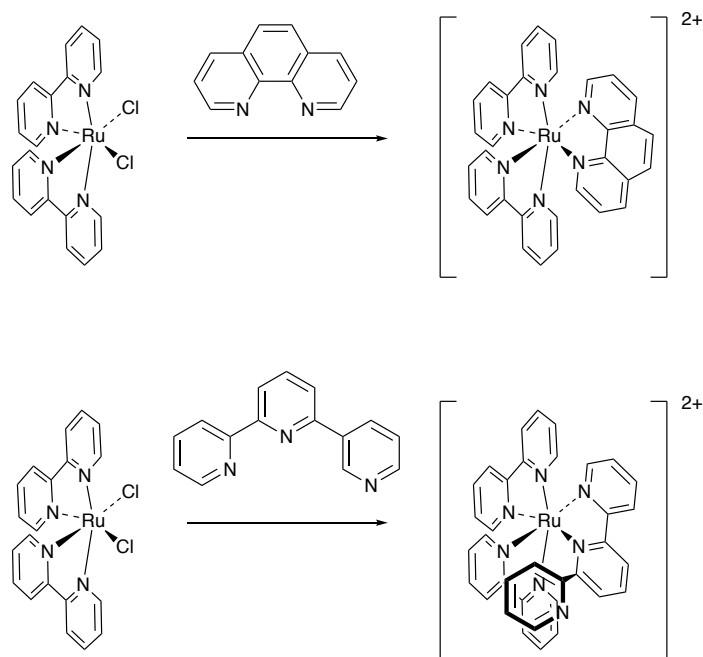


Figure 6 The reaction of $cis\text{-}[\text{Ru}(\text{bpy})_2\text{Cl}_2]$ (two adjacent coordination sites occupied by labile chlorido ligands) with phen (two *cis*-nitrogen donors) gives $[\text{Ru}(\text{bpy})_2(\text{phen})]^{2+}$. In contrast, the metallosupramolecular coding for the reaction of $[\text{Ru}(\text{bpy})_2\text{Cl}_2]$ (two adjacent coordination sites occupied by labile chlorido ligands) with tpy (three *cis* nitrogen donors) is incommensurate; the tpy is forced to adopt a hypodentate tpy-20 bonding mode in $[\text{Ru}(\text{bpy})_2(\text{tpy-20})]^{2+}$ in which only two of the nitrogen donors are coordinated to the ruthenium.

Extending this concept brings us into some core metallosupramolecular chemistry. The classical expectation of qtpy (Figure 2) is that it would act as a planar tetradentate ligand, and if the recognition features are correct, this is indeed what happens. The complex cations $[\text{Pd}(\text{qtpy})]^{2+}$ (40) and $[\text{Pt}(\text{qtpy})]^{2+}$ (41,42) both exhibit this bonding mode (Figure 7). Nevertheless, it is now possible to envisage a range of bonding modes for qtpy (Figure 5 which will give rise to a rich metallosupramolecular

chemistry. The key observation here is that the four potential nitrogen donor atoms can be partitioned in a variety of ways. It is this partitioning of donor sets that integrates the metal-binding domain description into the body of metallosupramolecular chemistry.



Figure 7 In the complex cations (a) $[\text{Pd}(\text{qtpy})]^{2+}$ and (b) $[\text{Pt}(\text{qtpy})]^{2+}$ the qtpy ligand functions as a planar tetradentate donor.

2.3.1 Partitioning metal-binding domains in polydentate ligands

In Section 2.4 we will describe how an understanding of the partitioning of polydentate ligands into discrete metal-binding domains allowed the development of the metallosupramolecular chemistry of helical systems. In that work we historically used descriptions such as [2+2] to describe the partitioning of a tetradentate ligand into two bidentate metal-binding domains. In this short section, we present a more refined version of this system which has a universal application. We introduce this notation not to replace the IUPAC kappa (43) nomenclature, but to use a shorthand

notation that is easy to define and interpret, neither of which are attributes of this particular aspect of the IUPAC system.

Figure 8 presents the possible coordination modes of 2,2'-bipyridine and 2,2':6',2''-terpyridine. If we consider 2,2'-bipyridine, it can act as a chelating bidentate, as a monodentate ligand with one non-coordinated pyridine, or as a bridging ligand connecting two different metals. We have developed the simple notation to describe the coordination quotient; the ligand is addressed sequentially along the chain and the end with the highest denticity is identified. In the case of bpy, the chelating mode has a denticity of 2 and the descriptor (2) suffices. For a hypodentate bpy ligand, the description becomes (10) – one nitrogen is coordinated and one is free. In the bridging mode, the descriptor is simply (1,1). In formulae we try to avoid a proliferation of brackets, and so the complex $[\text{MeHg}(3,3'\text{-Me}_2\text{bpy-10})](\text{NO}_3)$ (44) contains a monodentate 3,3'-dimethyl-2,2'-bipyridine ligand. Free ligands will always be represented by the quotient (0); the notation (0,0) for bpy is redundant as all donor atoms are non-coordinated by definition.

Applying this nomenclature to tpy, we immediately see a total of eight coordination modes. The classical tridentate chelating mode is denoted (3), but we now see a series of other possibilities including the hypodentate (20) mode that we discussed above. As we will see in the next section, modes such as tpy-21 and qtpy-22 are critical for the development of molecular helicity.

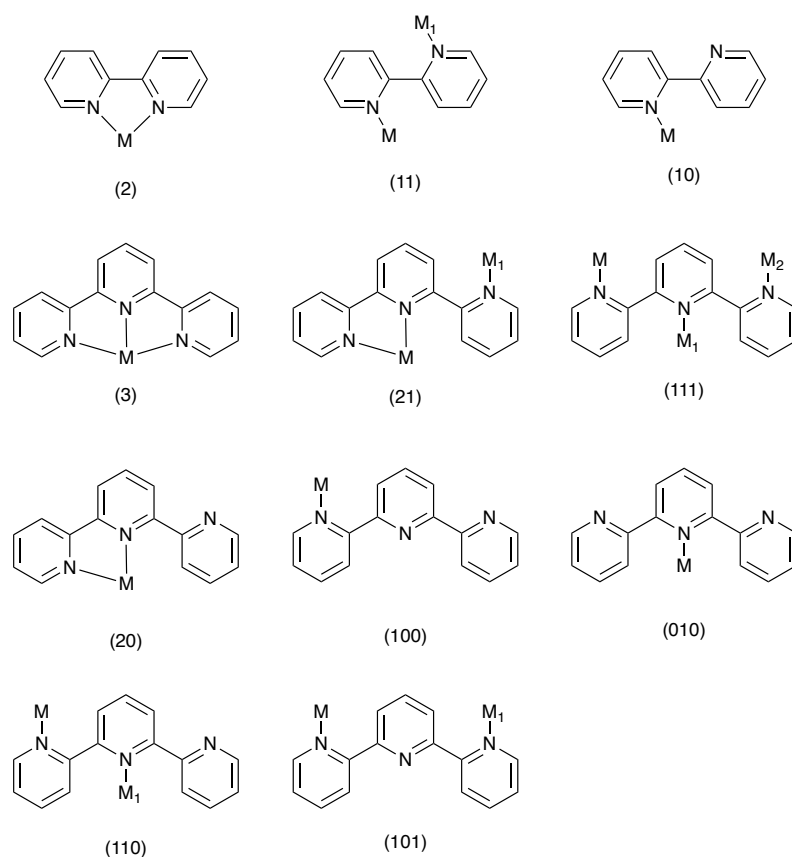


Figure 8 The possible bonding modes of bpy and tpy ligands. As for qtpy in Figure 5, modes in which a nitrogen donor bonds to two metal centres are omitted as they are a degenerate representation of the modes above. The metal centres M, M₁, M₂ and M₃ may be the same or different.

2.3.2 Symmetrical partitioning of metal-binding domains in helical metallosupramolecules

Just as the time came for the Walrus "to talk of many things" (45), so has the time arrived for us to talk of helicates. Numerous excellent reviews exist on this topic (12,46,47,48,49,50) and the aim here is to show how the concepts of metal-binding domains and their partition in a polydentate ligand combine with the precepts of

metallo-supramolecular chemistry to rationalize their formation. Our own modest contribution centred upon the use of oligopyridines and the reader is referred to the review literature cited above to place our work in the context of the wealth of elegant synthetic chemistry, in particular the paradigm-breaking contributions from the Strasbourg school. In this section, we only consider oligopyridine ligands without flexible spacers between the metal-binding domains.

We commence by considering the (22) coordination mode of qtpy and combining with a metal centre with four available coordination sites. Conceptually we can match the qtpy-22 with two metal ions to form a dinuclear complex of $\{M_2(qtpy-22)\}$ stoichiometry (Figure 9). However, each metal centre still has two additional coordination sites and the formation of an $\{M_2(qtpy-22)_2\}$ driven by multiple chelating interactions in which two bpy metal-binding domains are bound to each metal centre is reasonable. The partitioning of the qtpy-22 into two bpy domains also defines the coding at the metal centre, as shown at top of Figure 9. A square-planar metal centre is not compatible with the ligand coding (Figure 9a), but a tetrahedral centre, coupled with a twisting about the bond linking the two bpy metal-binding domains in the qtpy, leads to a novel dinuclear double-helical complex.

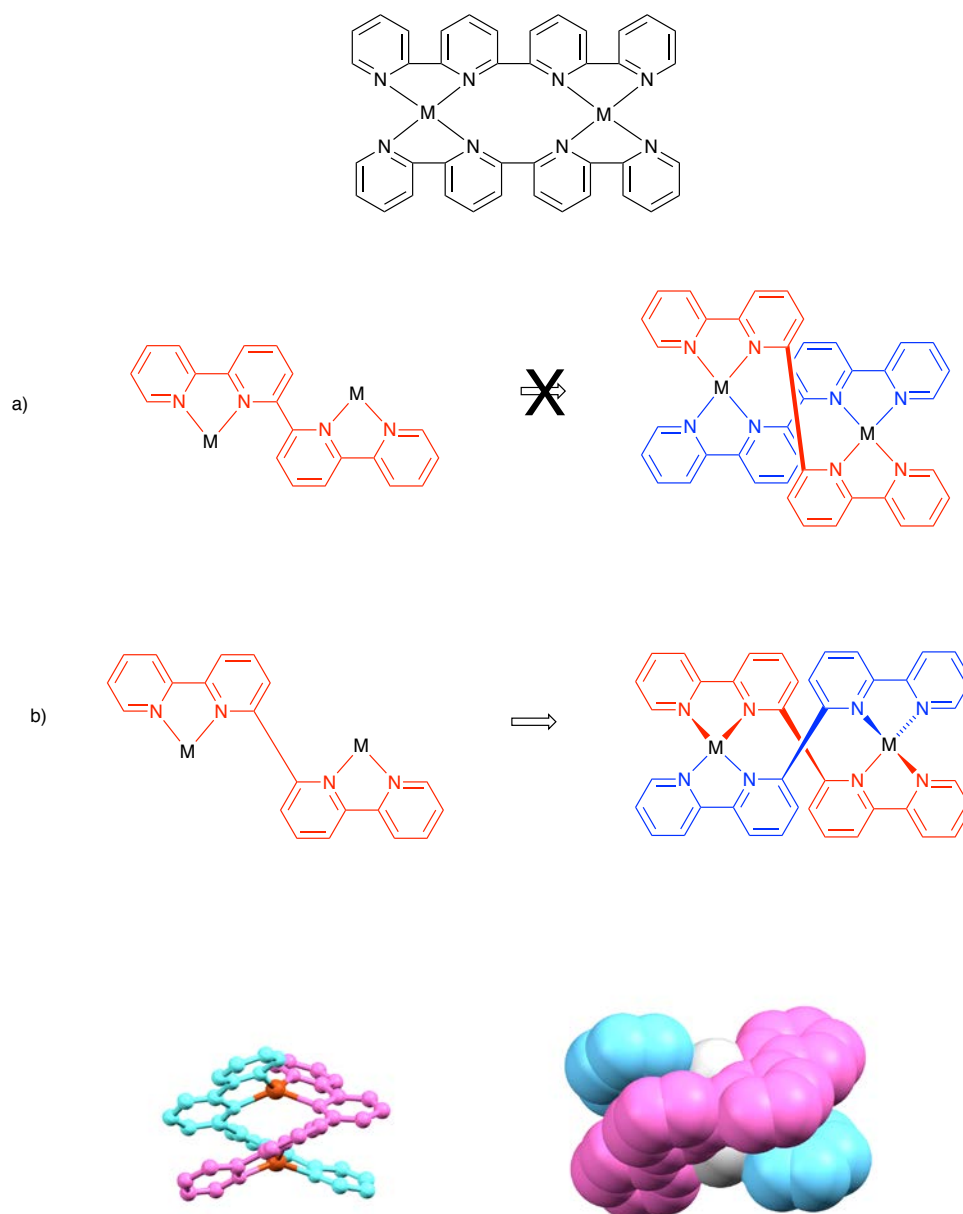


Figure 9 An array of two qtpy ligands can be divided into four bpy metal-binding domains which are commensurate with two four-coordinate metal centres. The coding in the qtpy-(22) ligand excludes a) square-planar metal centres but b) predicates two tetrahedral metal centres which in turn requires a rotation about the C-C bond linking the two bpy metal-binding domains. Figures 9c and 9d show different representations of the double-helical complex cations $[\text{Cu}_2(\text{qtpy})_2]^{2+}$ and

$[\text{Ag}_2(\text{qtpy})_2]^{2+}$ respectively. Hydrogen atoms have been omitted and the two ligand strands have been coloured for clarity.

In reality, simply reacting copper(I) or silver(I) salts with qtpy results in the formation of the dinuclear double-helical complexes $[\text{Cu}_2(\text{qtpy})_2]^{2+}$ and $[\text{Ag}_2(\text{qtpy})_2]^{2+}$ respectively (42,51). The helical structure is achieved primarily by twisting about the interannular C-C bond between the bpy metal-binding domains, with angles between the least squares planes of the metal-binding domains of 53.03 and 52.70° in the silver complex and 45.85° in the copper complex. The subtlety of the metallosupramolecular approach is well illustrated here; at the first level, the matching of the coding for the metal-binding domains and the metal centres leads to the gross structure, but second level factors such as the size of the metal ion further modulate the fine details.

It is worth noting here that we have also crossed the kinetic divide in addressing this aspect of metallosupramolecular chemistry. The hypodentate concept was developed at the beginning of Section 2.3 in the context of a kinetically inert d^6 metal centre, predicated upon the idea that chelating ligands "stay stuck". The products of the reactions are thus kinetic products. In the use of labile copper(I) or silver(I) cations we move into the world of spontaneous self-assembly in which metal-ligand bonds are made and broken many times in the course of the reaction and the products are in a thermodynamic minimum.

Using the analysis presented above, it is natural to ask if the metal-binding domain analysis of qtpy presents other possible modes? In principle, an array of three qtpy

ligands, each sub-divided into two bpy metal-binding domains could also bind two six coordinate metal centres (Figure 10a). In practice the steric interactions are too great and this mode has not been observed in qtpy itself. Nevertheless, introducing a spacer between the bpy metal-binding domains relieves these interactions and ligand **5** forms the triple-helical cation $[\text{Fe}_2(\mathbf{5})_3]^{4+}$ (Figure 10) (52). The introduction of spacers increases the complexity of the system, a good example being seen in the formation of systems possessing variable types of helical chirality (53). In general, the greater the flexibility in the spacer, the fuzzier the self-assembly algorithm becomes. This is not always disadvantageous, as a rigidly defined algorithm tends towards a binary response to self-assembly – it either works or it does not! In contrast, flexibility in the ligand allows adjustments in the distribution of the metal-binding domains to give the best fit to the best algorithm. An early example is seen with the chiralized ligand **6** (Figure 10) in which the bpy metal-binding domains are linked through the 6- rather than the 4-positions; this precludes the formation of a trinuclear triple helicate and the six metal binding domains partition into three sets coded for a tetrahedral metal centre and results in the formation of the trinuclear cyclic helicate $[\text{Cu}_3(\mathbf{6})_3]^{3+}$ (Figure 10b) in addition to the double-helicate (54). The field of cyclic helicates is evolving and the reader is referred to the review literature for an overview of this fascinating area (4653).

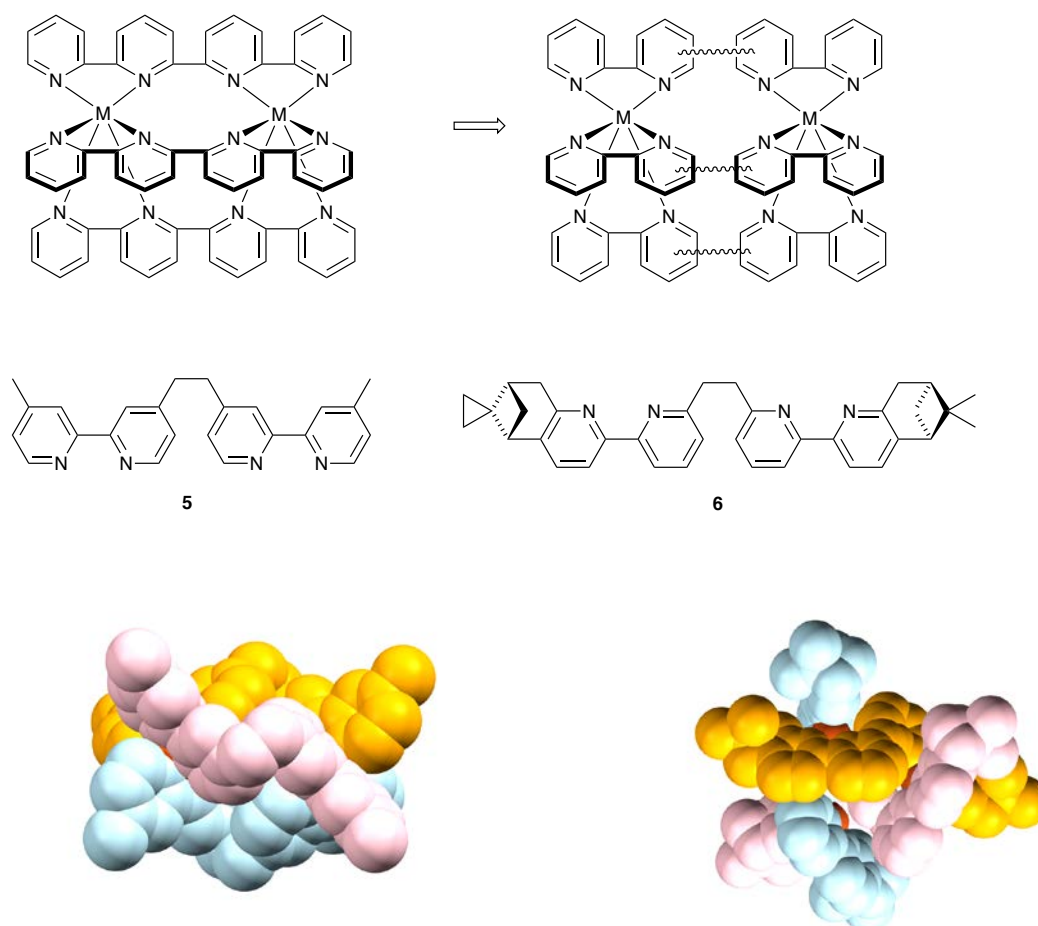


Figure 10 An array of three qtpy ligands can be divided into six bpy metal-binding domains which are commensurate with two six-coordinate metal centres. To observe this coding, it is necessary to introduce a spacer between the bpy metal-binding domains as in the ligand **5** which forms the trinuclear triple helicate $[\text{Fe}_2(\mathbf{5})_3]^{4+}$. In contrast, the ligand **6** can also form a trinuclear cyclohelicate $[\text{Cu}_3(\mathbf{6})_3]^{3+}$ which also satisfies the coding of two bpy metal-binding domains per copper centre. Hydrogen atoms have been omitted and the ligand strands have been coloured for clarity.

The oligopyridine sexipy can be subdivided into various metal-binding domains, of which the most symmetrical are the 222 and 33 modes, which exhibit three bpy or

two tpy metal-binding domains respectively (Figure 11) (55,56). There is good evidence for the formation of complexes of stoichiometry $[\text{Cu}_3\text{L}_2]^{3+}$ with spy-222 ligands and double helical complexes $[\text{M}_2\text{L}_2]^{4+}$ with spy-33 ligands have been structurally characterized with $\text{M} = \text{Fe}$ (57), Cd (58,59), Cu (60), Zn (61,62), Co (63). The coordination chemistry of the oligopyridines higher than spy has been intensively investigated by Potts (64,65) and others (57,61).

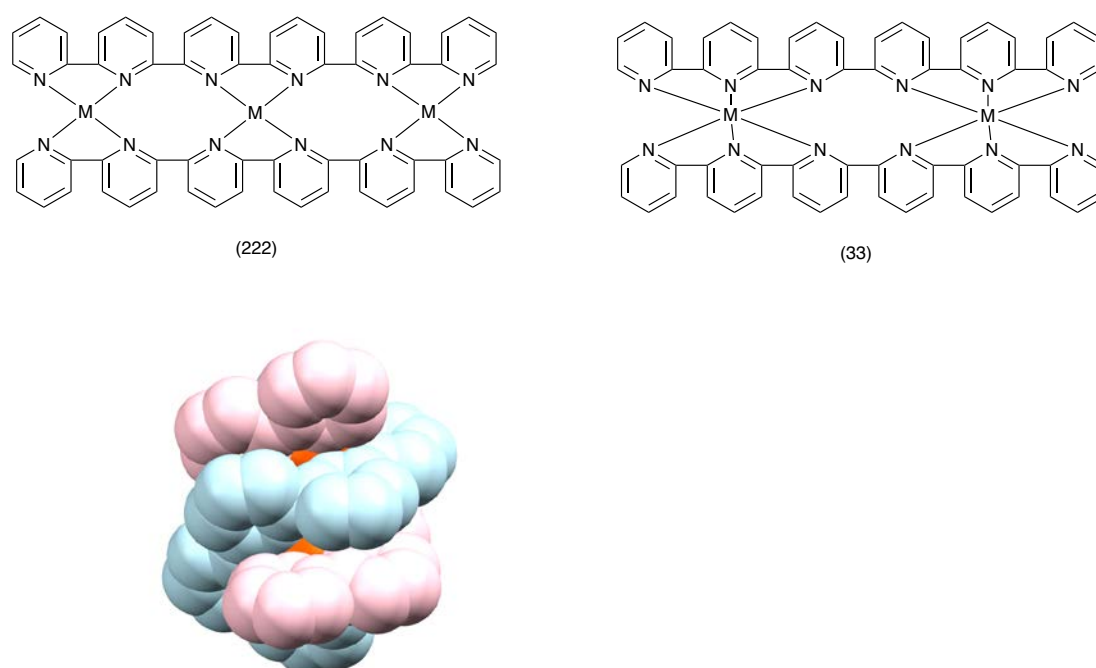


Figure 11 The ligand spy could be partitioned into three bpy metal-binding domains (222) or two tpy metal-binding domains (33). An array of two spy-222 ligands will bind three tetrahedral metal centres in a double helical structure whilst two spy-33 ligands will bind two octahedral metals in a double helix. The complex $[\text{Fe}_2(\text{spy})_2]^{4+}$ is a double-helical species in which each of the two spy-33 ligands present a tpy metal-binding domain to each metal. Hydrogen atoms have been omitted and the two ligand strands have been coloured for clarity.

2.3.3 Asymmetrical partitioning of metal-binding domains in helical metallocupramolecules

It is now instructive to consider oligopyridines with odd numbers of pyridine rings, of which tpy is the prototype. Is it possible to partition tpy ligands into bpy and py metal-binding domains? Some limiting structures for a complex of stoichiometry $[M_2L_2]^{n+}$ are presented at the top of Figure 12. Somewhat to our surprise, the reaction of copper(I) salts with 6,6'-Ph₂tpy resulted in the formation of a dinuclear double helix of type I (Figure 12a) (66); it has also been found that tpy (67) 6,6''-Ph₂-4,4''-(SMe)₂tpy (68) and a range of chiral tpy ligands (69,70,71,72) all form double-helical dinuclear $[Cu_2L_2]^{2+}$ structures closest to type III (although 6,6''-Ph₂-4,4''-(SMe)₂tpy (68) can also be described as closer to type I).

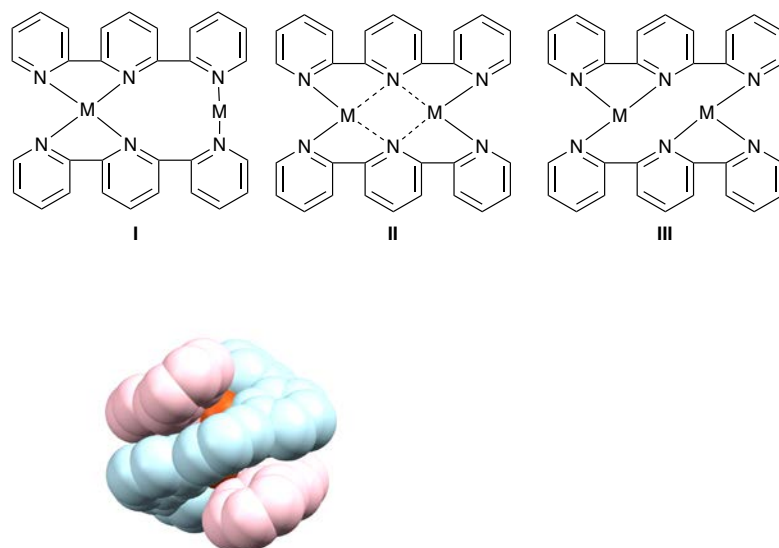


Figure 12 The ligand tpy could form dinuclear $[M_2L_2]$ complexes by partitioning into bpy and py metal-binding domains in tpy-21 as in structure types I and III. In reality,

the M-N distances are not clear cut and the distinction between structure types II and III is blurred. The complex $[\text{Cu}_2(6,6''\text{-Ph}_2\text{-tpy})_2]^{2+}$ is a double-helical species in which the two tpy-21 ligands giving a complex of structure type I. Hydrogen atoms have been omitted and the two ligand strands have been coloured for clarity.

For the double-helical $[\text{M}_2\text{L}_2]^{2+}$ silver complexes with ligands including 4,4',4''-tBu₃tpy (73, 74), 4'-Phpty (75, 76), 6,6''-Me₂tpy (77), 6-bornyloxytpy (70,71), structures of type I (73,74,75,77), type II (71,77) and type III (76,77) are adopted with the counter-ion and any additional coordinated ligands playing a critical role. It is of interest that there are short Ag...Ag interactions between dinuclear double helices in $[\{\text{Ag}_2(\text{L})_2\}_2]^{4+}$ with L = 4'-Phpty (2.880 Å) (75), L = 6-bornyloxytpy (3.107, 3.157 Å) (70).

We finish this section with a short discussion of the behaviour of the pentadentate ligand qpy (Figure 2). This is not the place to fully review the behaviour of this ligand, which has been discussed in detail elsewhere, but rather because it illustrates the exquisite subtlety of metallosupramolecular chemistry. We originally considered qpy because the potential pentadentate donor set was formally the same as that found in **3** and **4** (Figure 13). The experience with other oligopyridines suggests that qpy might not only adopt a qpy-5 mode analogous to the macrocycles discussed earlier, but also could partition into discrete metal-binding domains. Inspection suggests that the qpy-32 mode, in which tpy and bpy metal-binding domains are generated is likely to be commensurate with four and six-coordinate metal ions. A near-planar qpy-5 mode is exhibited in five coordinate $[\text{Ag}(\text{qpy})]^+$ (78) and in the seven coordinate complexes $[\{(\text{H}_2\text{O})(6,6'''\text{-Me}_2\text{qpy})\text{Mn}\}_2\text{Cl}]^{3+}$ (79), $[(\text{qpy})\text{Fe}(\text{MeCN})_2]^{2+}$ (80), $[(4',4'''\text{-$

$\text{Ph}_2\text{qpy})\text{Fe}(\text{MeCN})_2]^{2+}$ (80), $[\{(\text{H}_2\text{O})(\text{qpy})\text{Fe}\}_2\text{O}]^{2+}$ (81), $[\text{Co}(6,6''''\text{-Me}_2\text{qpy})(\text{ONO}_2)_2]$ (82), $[\text{Co}(4',4''''\text{-(EtS)}_2\text{qpy})\text{Cl}_2]$ (83,84), $[\text{Co}(4',4''''\text{-(4-ClC}_6\text{H}_5)_2\text{qpy})(\text{H}_2\text{O})(\text{MeOH})]^{2+}$ (85,86), $[\text{Cd}(6,6''''\text{-Me}_2\text{qpy})(\text{OCIO}_3)_2]$ (87) and $[\text{Re}(\text{qpy})\text{Cl}_2]^+$ (88).

To summarize a great deal of work, qpy ligands tend to partition in the qpy-32 bonding mode and for dinuclear double helicates. The typical partitioning is to bind a six-coordinate metal by two tpy metal-binding domains leaving the remaining two bpy-metal domains free for the second metal. Homonuclear systems are known in which the second site is occupied by a four-, five- or six-coordinate metal centre, with the ancillary ligands when the coordination number is greater than four. Dinuclear double helicates have been structurally characterized with qpy and a variety of substituted ligands and the vast majority adopt structure I (Figure 14). Structure type I is found in the homonuclear double helicates containing Cu(II) (89,90,91), Co(II) (92,93), Ni(II) (60,86,94), Ru(II) (95). Reduction of the Cu^{II}_2 double helicate to the $\text{Cu}^{\text{II}}\text{Cu}^{\text{I}}$ level gives a perfect match to the six and four coordinate binding cavity is the array of two qpy-32 ligands (Figure 14a) (87,90,91,96). In the case of Co^{II}_2 double helicates, donor solvents or good donor ancillary ligands or counterions establish an equilibrium with seven-coordinate mononuclear species $[\text{Co}(\text{qpy-5})\text{X}_2]^{n+}$ and we will return to this observation shortly.

We had expected that the structure type II would be favoured by copper(II) in view of the preference of this metal for a five-coordinate coordination environment with one tpy and one bpy metal-binding domain (97), but this mode has not been structurally characterized for copper(II). Rather unexpectedly, double helicates with structure type II are found in $[\text{Pd}_2(\text{qpy-32})_2][\text{PF}_6]_4$ (41) (Figure 14b), $[\text{Ag}_2(6,6''''\text{-Me}_2\text{-4',4''''\text{-Ph}_2\text{qpy-}$

$32)_2][ClO_4]_2$ and $[Ag_2(6,6''''-Me_2qpy-32)_2][ClO_4]_2$ (98) whereas 4',4''''-Fc₂qpy forms a type I double helicate with silver triflate (albeit with one long Ag-N bond) (99).

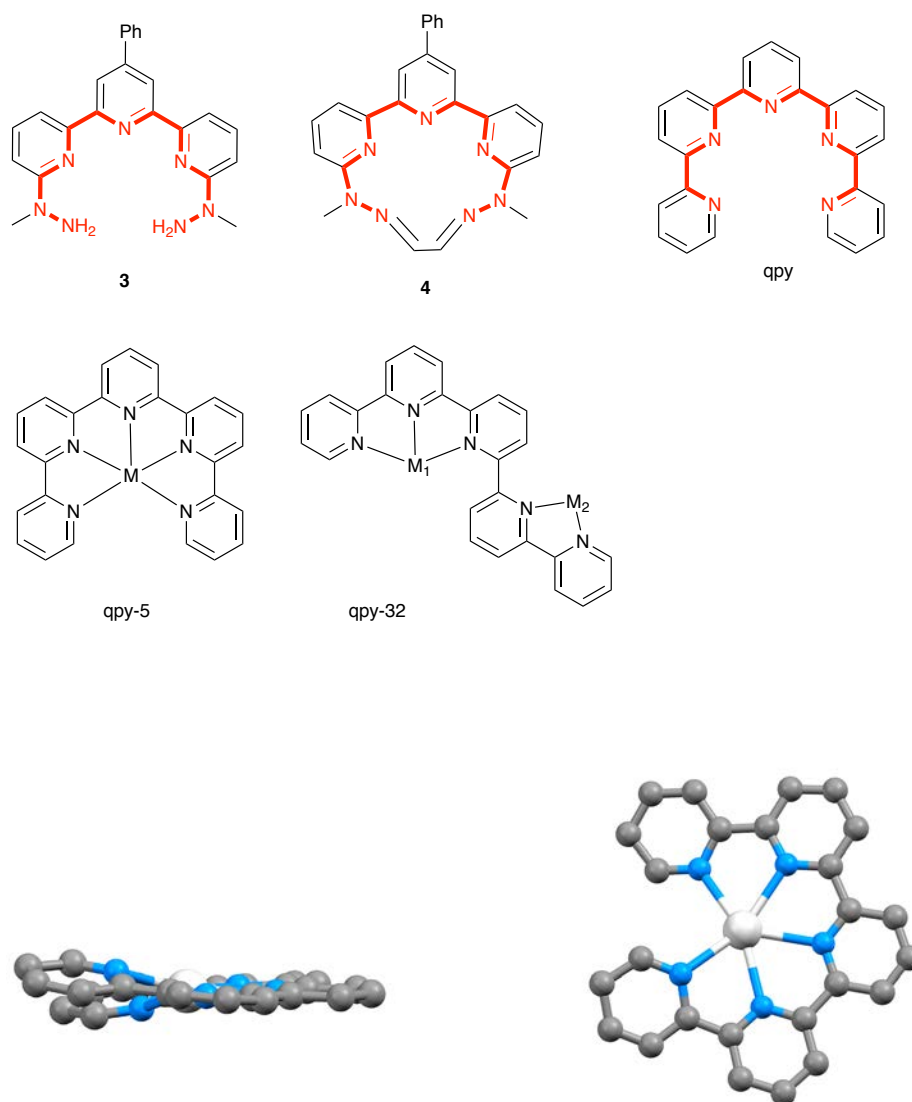


Figure 13 The pentadentate donor set of qpy has a formal similarity to that of the macrocycle 4 and the precursor 3. The analogy to the macrocycle would require the bonding mode qpy-5, which is found in the complex $[Ag(qpy)][PF_6]$. Hydrogen atoms have been omitted for clarity.

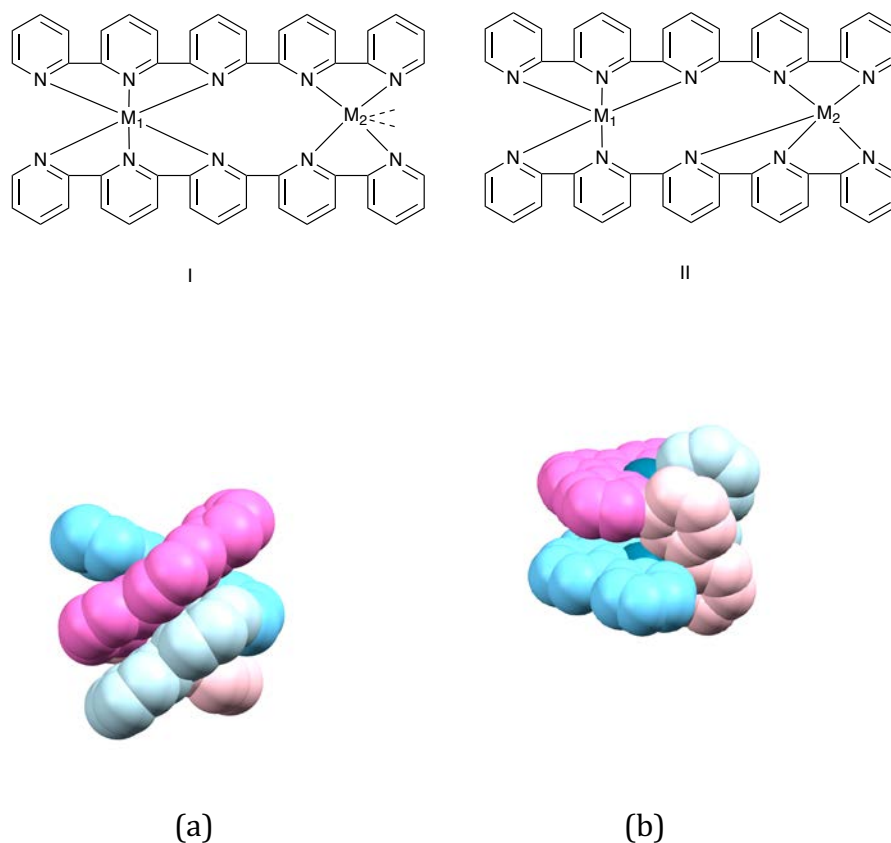


Figure 14 Two ways in which qpy-32 ligands can form a dinuclear double helicate with two metal ions. In structure type **I**, one metal binding site is preorganized with two tpy metal-binding domains for an octahedral metal centre and the second site has two bpy metal-binding domains and can accommodate four-, five- or six-coordinate metal centre as found in (a) $[\text{Cu}^{\text{I}}\text{Cu}^{\text{II}}(\text{qpy-32})_2]^{3+}$. The alternative structure type **II** with two five coordinate metal centres is found in (b) $[\text{Pd}_2(\text{qpy-32})_2]^{4+}$. Hydrogen atoms have been omitted and the two ligand strands have been coloured for clarity. In each case, the tpy metal-binding domain is shaded darker than the bpy metal-binding domain.

We conclude this section by showing the power of metallosupramolecular chemistry.

When $[\text{Co}_2(\text{qpy-32})_2(\text{OAc})]^{3+}$ is dissolved in MeCN, the mononuclear complex

$[\text{Co}(\text{qpy-5})(\text{MeCN})_2]^{2+}$ is formed in solution (92). The complex cation $[\text{Ag}(\text{qpy-5})]^+$ is five-coordinate (78). The preferred coordination sphere of silver(I) is four-coordinate tetrahedral and that of cobalt(II) is six-coordinate octahedral. This prompted us to investigate the reaction of these two species in the hope that they would form a heterodinuclear double helicate with qpy-32 ligands supporting the cobalt with two tpy metal-binding domains and the silver bound to two bpy metal-binding domains. This was indeed the case and the structure of $[\text{CoAg}(\text{qpy-32})_2]^{3+}$ is shown in Figure 15 (100). A similar logic allowed the preparation of $[\text{Ni}^{\text{II}}\text{Cu}^{\text{I}}(\text{qpy-32})_2]^{3+}$ in which the copper(I) is in the cavity created by two bpy metal-binding domains (101).

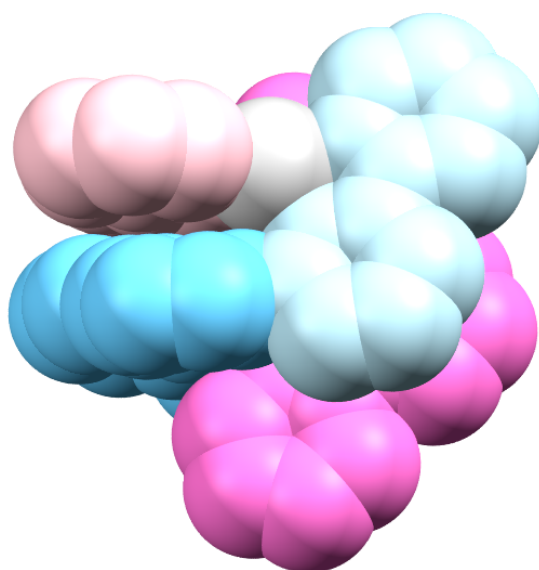


Figure 14 The heterodinuclear double helicate $[\text{CoAg}(\text{qpy-32})_2]^{3+}$ is formed from the reaction of $[\text{Co}(\text{qpy-5})(\text{MeCN})_2]^{2+}$ with $[\text{Ag}(\text{qpy-5})]^+$. Hydrogen atoms have been

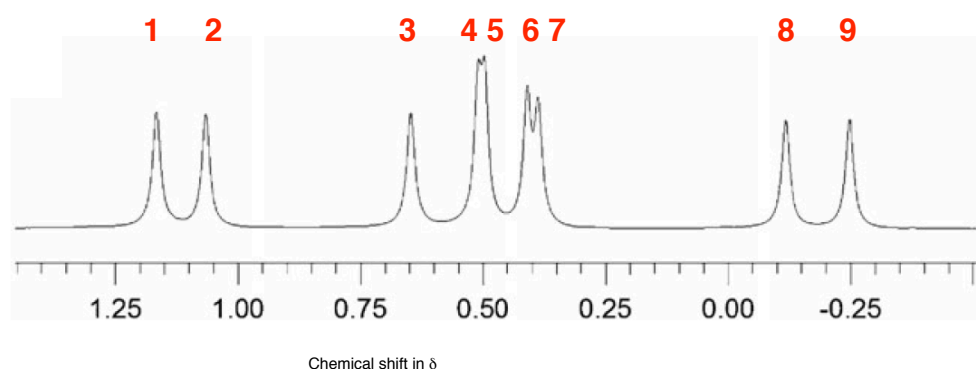
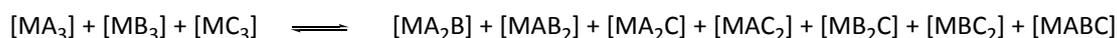
omitted and the two ligand strands have been coloured for clarity. In each case, the tpy metal-binding domain is shaded darker than the bpy metal-binding domain.

2.4 From pure compounds to libraries

In the course of the studies described above, we recognized that labile complexes could be used to generate equilibrium mixtures of metal complexes. In the mid to late 1990's the search for new pharmaceutically active compounds moved from linear synthesis of individual compounds to the generation of combinatorial libraries and the selection of active lead compounds from these arrays (102,103). The method was developed using irreversible covalent bond formation methodologies, in particular for peptide and nucleotide derivatives. If the key bond-formation reactions are reversible, the reversible reaction of building blocks under thermodynamic control generates a dynamic combinatorial library (104, 105, 106). In organic chemistry, dynamic combinatorial libraries are typically prepared using imines or disulfides. The benefit of inorganic chemistry is that labile metal centres offer the opportunity of rapid ligand exchange in species in which the bond is at the same time strong, an idea first established by Lehn and co-workers (107).

Consider two labile complexes $[MA_3]$ and $[MB_3]$ which can equilibrate through ligand exchange (Scheme 2). By mixing the two complexes $[MA_3]$ and $[MB_3]$ a library of four compounds could be obtained and by the further addition of $[MC_3]$ a library of ten complexes. If the ligands A, B and C have reactive substituents, then the new libraries could have different interactions with target substrates.

Statistical equilibration of a 1:1:1 mixture $[\text{MA}_3]$, $[\text{MB}_3]$ and $[\text{MC}_3]$ will give a 1:1:1:3:3:3:3:3:6 distribution of $[\text{MA}_3]$, $[\text{MB}_3]$, $[\text{MC}_3]$, $[\text{MA}_2\text{B}]$, $[\text{MAB}_2]$, $[\text{MAC}_2]$, $[\text{MA}_2\text{C}]$, $[\text{MB}_2\text{C}]$, $[\text{MBC}_2]$ and $[\text{MABC}]$. This has been established for exchange between the three complexes $[\text{Co}(\text{phen})_3][\text{PF}_6]_2$, $[\text{Co}(\text{bpy})_3][\text{PF}_6]_2$ and $[\text{Co}(4,4'\text{-Me}_2\text{bpy})_3][\text{PF}_6]_2$; each chemically equivalent proton (for example the methyl in 4,4'- Me_2bpy) gives nine signals in the ^1H NMR spectrum (one for $[\text{Co}(4,4'\text{-Me}_2\text{bpy})_3]^{2+}$, two each for $[\text{Co}(4,4'\text{-Me}_2\text{bpy})_2(\text{phen})]^{2+}$ and $[\text{Co}(4,4'\text{-Me}_2\text{bpy})_2(\text{bpy})]^{2+}$, one each for $[\text{Co}(4,4'\text{-Me}_2\text{bpy})(\text{phen})_2]^{2+}$ and $[\text{Co}(4,4'\text{-Me}_2\text{bpy})(\text{bpy})_2]^{2+}$, and two from $[\text{Co}(4,4'\text{-Me}_2\text{bpy})(\text{bpy})(\text{phen})]^{2+}$) and this is exactly what is found in the spectrum of this mixture (108).



Scheme 2 The equilibration of a mixture of two or three homoleptic ML_3 complexes can generate a library of four or ten components respectively. In the case of a 1:1:1 mixture of labile $[\text{Co}(\text{phen})_3][\text{PF}_6]_2$, $[\text{Co}(\text{bpy})_3][\text{PF}_6]_2$ and $[\text{Co}(4,4'\text{-Me}_2\text{bpy})_3][\text{PF}_6]_2$ the expected set of nine signals of equal intensity for each ligand proton is observed. The 500 MHz ^1H NMR spectrum shows the nine signals for the methyl groups of the 4,4'-

Me₂bpy ligand in the library. Note that the paramagnetic d⁷ cobalt(II) centre results in a very large chemical shift range for the protons, allowing for the identification of the individual signals.

It was now possible to show that the distribution of complexes within a dynamic combinatorial library could be addressed through selective reaction of one of the components. The reaction of 2,2'-bipyridine-5-carboxaldehyde **5** with cobalt(II) salts generates a dynamic library containing the two components, the *mer* and *fac* stereoisomers of [Co(**5**)₃]²⁺. The three ligands in the *fac* complex are chemically and magnetically equivalent (Figure 16), whereas each ligand is chemically and magnetically unique in the *mer* isomer. Thus, for each unique proton in ligand **5**, four signals are expected in the ¹H NMR spectrum of the mixture of *mer* and *fac* stereoisomers of [Co(**5**)₃]²⁺, which is indeed observed (108). Furthermore, the dynamic nature of the library is established by the observation of exchange peaks in the EXCSY spectrum between all four signals arising from a given ligand proton, demonstrating the chemical exchange between the *mer* and *fac* stereoisomers. Finally, the amplification of the library was demonstrated by reaction with N(CH₂CH₂NH₂)₃ which can only react with the *fac* stereoisomer to form the capped complex **6**. reaction of the dynamic library with N(CH₂CH₂NH₂)₃ gives only the capped complex Y, and the *mer* stereoisomer is converted to *fac* as the *fac* form in turn is removed from equilibrium by condensation with the tris(amine).

One of our aims with this approach was to generate a multi-level combinatorial library, which would be labile and allow ligand exchange at the cobalt(II) level and after oxidation to kinetically inert d⁶ cobalt(III) would allow the system to be

"frozen". In practice, this approach was not successful, as rapid electron transfer between the cobalt(II) and cobalt(III) systems resulted in ligand scrambling. Nevertheless, it allowed us to make an interesting observation. A mixture of $[\text{Co}(\text{tpy})_2]^{3+}$ and $[\text{Co}(\text{tpy})_2]^{2+}$ is a self-exchange system with a rate of electron transfer of $50 \text{ M}^{-1}\text{s}^{-1}$ at room temperature (109,110). The ^1H NMR spectrum of a mixture of these two complexes exhibits two subspectra, one for $[\text{Co}(\text{tpy})_2]^{2+}$ which is paramagnetically shifted and one for $[\text{Co}(\text{tpy})_2]^{3+}$ which is diamagnetic. The ^1H NMR exchange spectrum shows cross peaks between the protons of the tpy ligands in $[\text{Co}(\text{tpy})_2]^{2+}$ with those in $[\text{Co}(\text{tpy})_2]^{3+}$. The *electron transfer* reaction between $[\text{Co}(\text{tpy})_2]^{2+}$ and $[\text{Co}(\text{tpy})_2]^{3+}$ interconverts cobalt(II) and cobalt(III) complexes and is detected by NMR spectroscopy as an apparent *chemical exchange* of $[\text{Co}(\text{tpy})_2]^{3+}$ and $[\text{Co}(\text{tpy})_2]^{2+}$ cations (111).

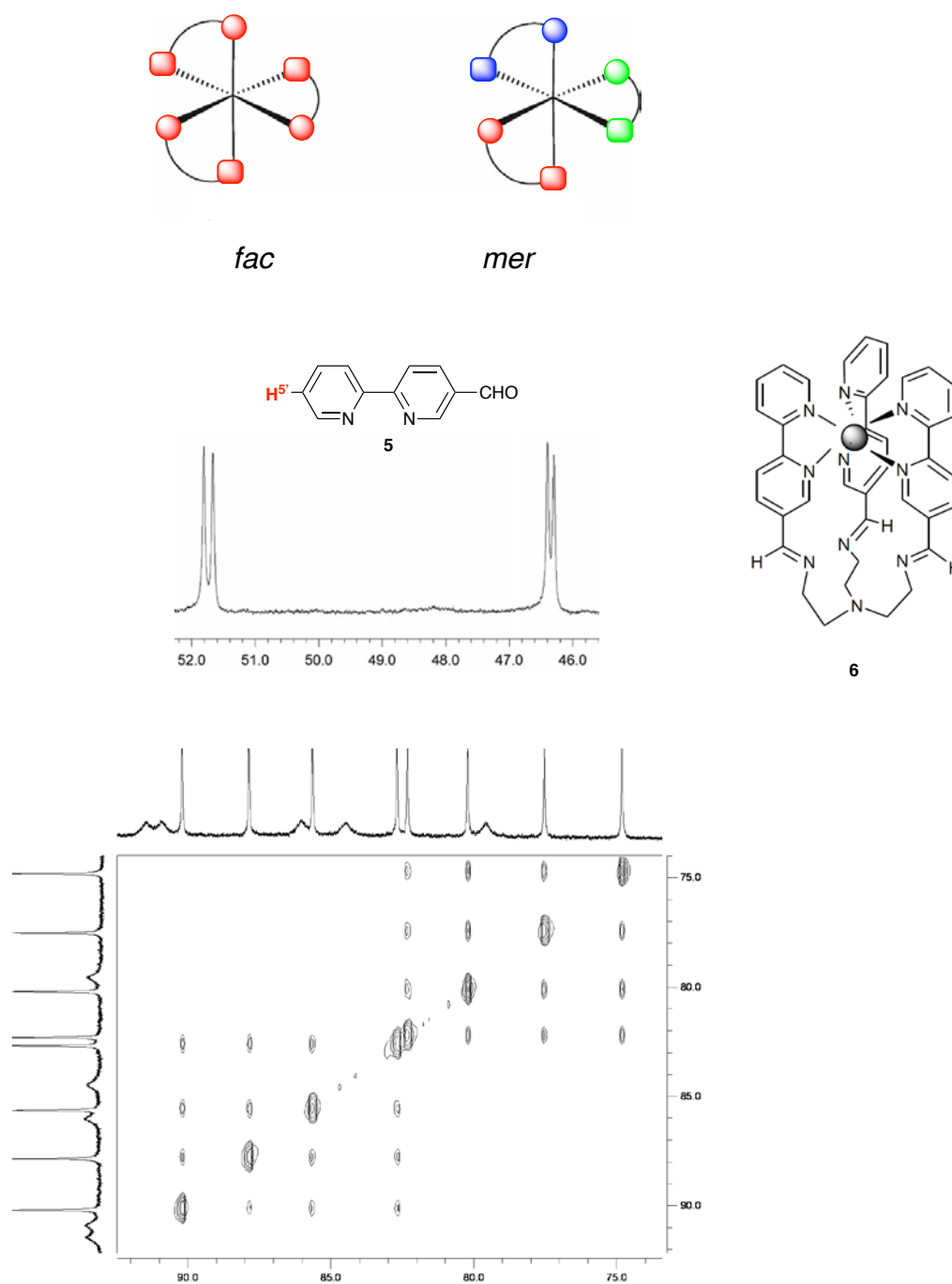


Figure 16 The equilibration mixture of *mer* and *fac* stereoisomers of $[Co(5)_3]^{2+}$ exhibits four signals in 1H NMR spectrum for each unique proton in the free ligand, as shown for the H5' proton. Once again, note that the paramagnetic d^7 cobalt(II) centre results in a very large chemical shift range for the protons. The dynamic nature of the library is established by the observation of exchange peaks in the

EXCSY spectrum between the four signals arising from each ligand proton. In the reaction of the *mer/fac* equilibrium mixture with $\text{N}(\text{CH}_2\text{CH}_2\text{NH}_2)_3$ only the *fac* stereoisomer can react to form the capped system **6**; as the *fac* isomer is removed to form the capped complex, the system re-equilibrates and eventually the only species present is **6**.

3 Supramolecular chemistry at surfaces

Why should we move from solution phase phenomena to surface binding? Our answer to this question lies in the origins of supramolecular chemistry. One of the driving forces in supramolecular chemistry was a desire to understand the complexities of biological assembly and replicate it in unnatural systems. How successful were we? A classical biological example of self-assembly is the tobacco mosaic virus (Figure 17). Under the correct conditions of pH, temperature and concentration, 2131 molecules of two different types (2130 molecules of a protein and one molecule of RNA) spontaneously assemble to form an active (virulent) virus (112). In this context, supramolecular chemistry is rather successful and the assembly of a discrete nanosphere from 72 component molecular species of two types (24 metal ions and 48 ligands) (113) or the construction of molecular Borromean rings in a single step from 18 components by the templated formation of 12 imine and 30 coordination bonds, generating three interlocked macrocycles about six zinc(II) centres (114) are only different from the tobacco mosaic virus in scale.

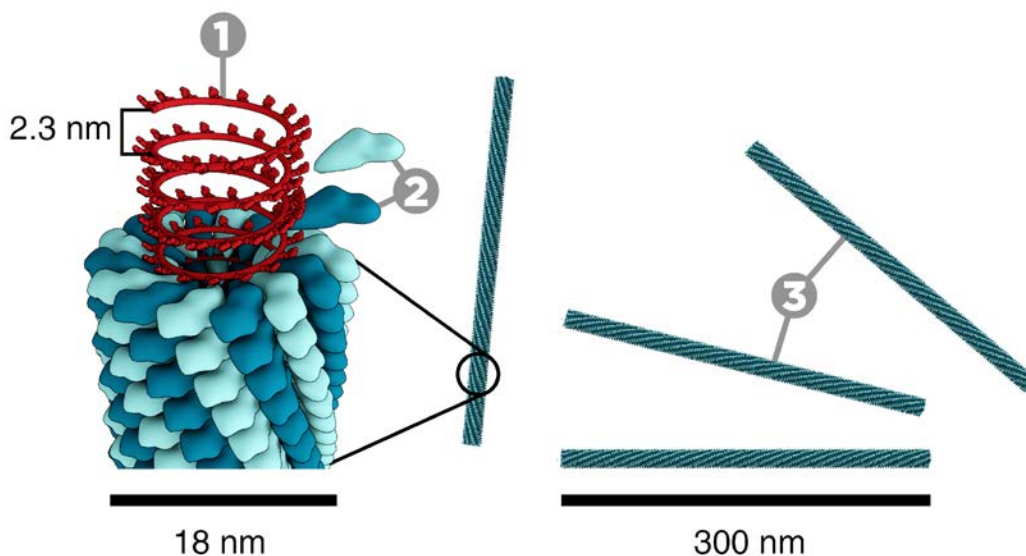


Figure 17 Under the correct conditions of pH, temperature and concentration, 2130 molecules of a protein and one molecule of RNA spontaneously assemble to form the active tobacco mosaic virus.

(https://en.wikipedia.org/wiki/Tobacco_mosaic_virus#/media/File:TMV_structure_full.png under creative commons licence).

We also see that this success is relative when we consider more complex biological machines. A stunning example of the precision and the complexity achieved in biology is seen in the structure of the core antenna-reaction centre complex (ttLH1-RC, Figure 18) of *Thermochromatium tepidum* in which over 100 components (cytochrome, L,M and H subunits of the reaction centre, 16 $\alpha\beta$ subunits of LH1 and some 80 cofactors) are precisely arranged to optimize energy and electron transfer in the overall functioning system. In contrast, synthetic chemistry is good at understanding the mutual interactions of two or three different types of molecule but cannot yet begin to approach the precision and complexity of biology. Why is this? This relates to a naïvety that some of us had at the beginning of supramolecular

chemistry – this naïvety was that biology worked in aqueous medium and therefore we could replicate biology in solution.



Figure 18 The core antenna-reaction centre complex (ttLH1-RC) of *Thermochromatium tepidum* in which over 100 components are precisely positioned.

In practice, the exquisite spatial control in ttLH1-RC is achieved by the use of phospholipid membranes as interfaces that support and enclose an aqueous medium and allow the precise management of the rates and thermodynamics of molecular transformations. As inorganic chemists, we asked ourselves what our organisational principle equivalent to the phospholipid membrane could be and furthermore what added value we might be able to bring with unnatural systems. We decided to concentrate upon the solid-fluid (gas or liquid) interface as a structure for the organization of multiple reactive species in a precise and defined manner. Our added value was that we would select solid materials with electronic properties which would

allow us to directly address molecular species at the interface by electron or energy transfer.

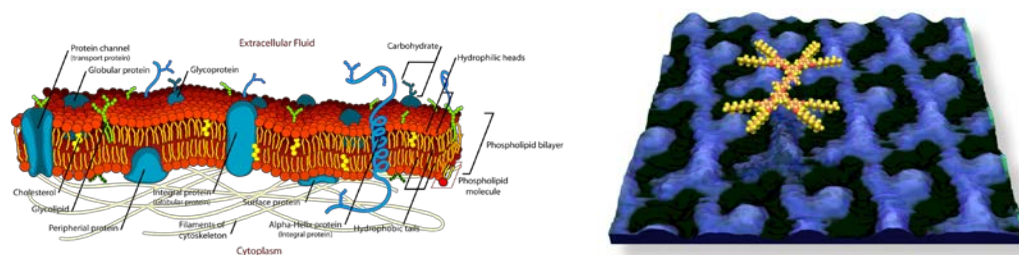


Figure 19 The naïve organisational model that lies at the basis of our research. We utilize the interface between solid and fluid as an organizational motif for beginning to address the hierarchical structuring of multiple species without the use of covalent bonding.

3.1 Overview of supramolecular interactions

In the earlier parts of this article, we have concentrated upon metal-ligand interactions for the control of supramolecular assembly and structure. However, in the course of these studies we were ever more aware that all of the forces of supramolecular chemistry worked together (or sometimes against each other) to achieve the final supramolecular structure.

The traditional forces of supramolecular chemistry include hydrogen bonding, hydrophobic and hydrophilic forces, van der Waals forces, π -interactions and electrostatic effects (115,116,117,118,119,120). In metallosupramolecular chemistry, electrostatic interactions can be of critical importance; the interaction between a metal centre and an anion can lead to short interactions which distort coordinated ligands or

even change the coordination number as the anion becomes coordinated. The studies of helicates discussed above revealed that face-to-face and edge-to-face π -interactions (*121, 122*) were abundant and probably responsible for the fine-tuning of the structures. Inspired by these observations, we commenced a series of investigations involving supramolecular organization at surfaces. These were predicated upon the preparation of materials rich in aromatic rings and investigating their interactions with highly oriented pyrolytic graphite using scanning tunnelling microscopy (STM) in the naïve assumption that a dominant self-assembly motif would be face-to-face π -interactions.

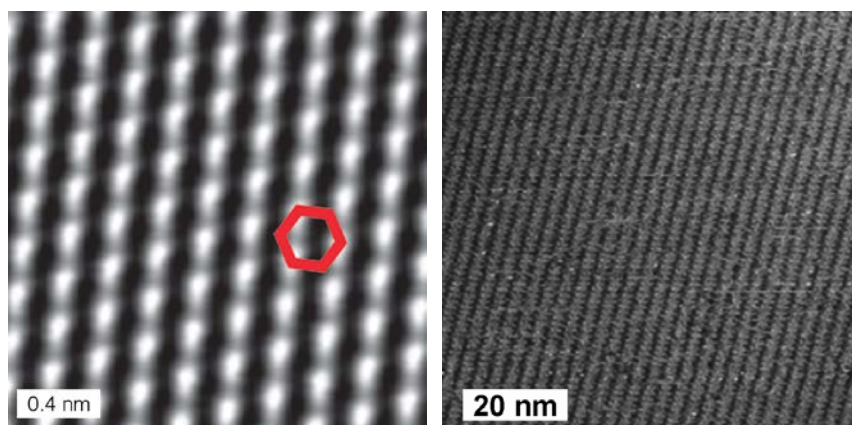
3.2 Self-assembly at surfaces

In the first studies in this area, we used highly oriented pyrolytic graphite (*123,124,125,126*) which is a substrate with an atomically flat surface, with a well-defined structure comprising a graphitic surface (Figure 20a). The technique of choice was STM (*127*). A conducting tip, ideally atomically dimensioned at the point, is scanned over a conducting surface at distances less than 1 nm, with the distance being controlled by the tunnelling current between the tip and the surface. This is a quantum mechanical effect, with current flowing between two electrodes through a thin insulator or a vacuum gap, and decaying by a factor of ≈ 450 over one atomic radius. The tunnelling current flows from the atomic apex of the tip apex to single atoms at the surface, inherently allowing atomic resolution. The technique is ideally suited for the investigation of monolayers of molecules on atomically flat surfaces. One always needs to be aware that STM plots a surface of constant tunneling probability (strictly

related to the local density of states near the Fermi level), although this is often interpreted atomistically as the real topography of the surface.

We approached this technique as chemists rather than physicists – put bluntly, we wanted to use the technique under ambient conditions of temperature and pressure studying multiple samples per day, rather than studying single samples for extended periods at millikelvin temperatures in ultra high vacuum. In other words, could we use STM as a spectroscopic or structural technique? Furthermore, we used wet chemical methods for the preparation of the monolayers, typically solution casting or direct measurement through liquid at the solid liquid interface (128).

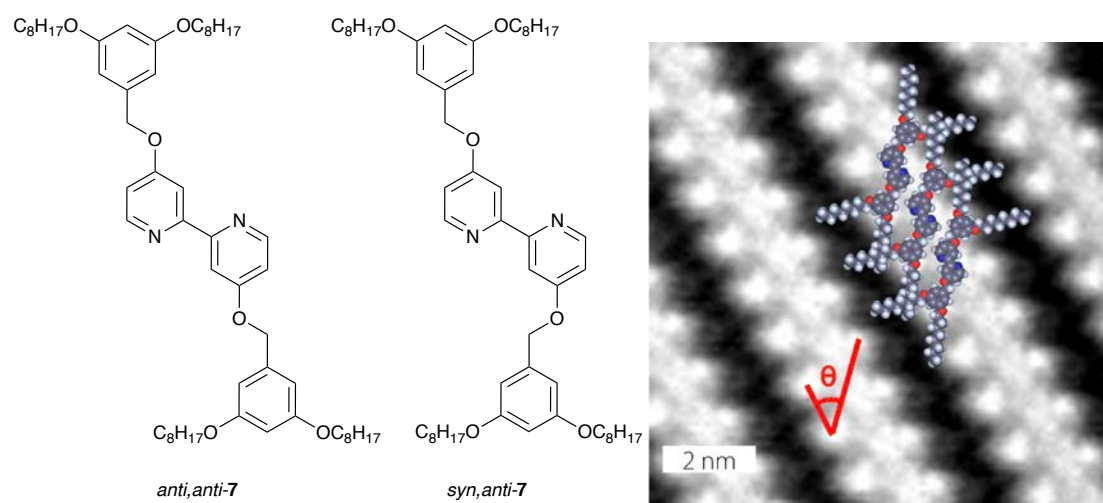
We decided to investigate Fréchet-type dendrimers (129,130) and their conjugates with oligopyridines. These were selected as they contained a large number of aromatic rings which were expected to optimise organization through face-to-face π -interactions with the graphitic surface. Initial studies with the first generation functionalized by ligand **7** allowed the molecules to be imaged with sub-molecular resolution (Figure 20b) (131). In this work we often observed multiple domains on the surface and realised that STM could be used as a tool to perform stereochemical analysis; Figure 21 shows the molecular resolution images and molecular fitting of the monolayers formed from the *anti,anti*- and *syn,anti*- conformations of **7** (131,132).



(a)

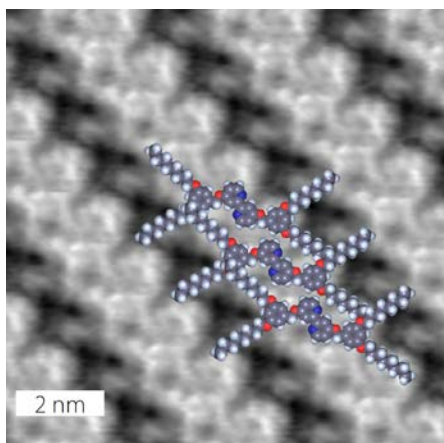
(b)

Figure 20 (a) An STM image of a 5 nm x 5 nm area of an HOPG surface. A single hexagon of the graphitic layer is marked in red - only three carbon atoms (out of the six in the hexagon) are visible (133) and (b) an image of a monolayer of compound **7** on HOPG.



(a)

(b)



(c)

Figure 21 (a) *anti,anti-* and *syn,anti-* conformations of **7** (b) and STM images of HOPG monolayers of molecular resolution images and molecular fitting of (b) the *anti,anti-* and (c) the *syn,anti-* conformations.

These studies were then extended to second generation dendrimers and their precursors and a typical example is seen in Figure 22, where in the monolayer molecules of the second-generation alcohol **8** form trimeric clusters on the surface (134). In the course of these studies we became increasingly aware that our original vision of monolayers dominated by face-to-face π -interactions of the dendron with the HOPG surface was naïve and that dominant forces were associated with the binding of the interdigitated alkyl chains with the HOPG surface. In subsequent studies, we investigated the influence of detailed molecular structure on the self-organisation properties (135,136,137,138,139,140).

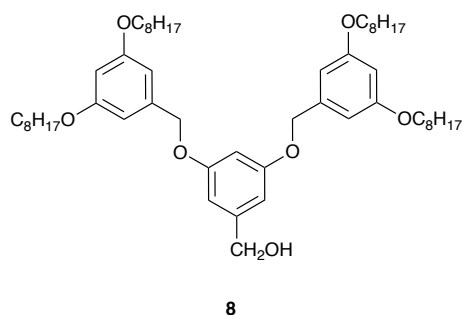
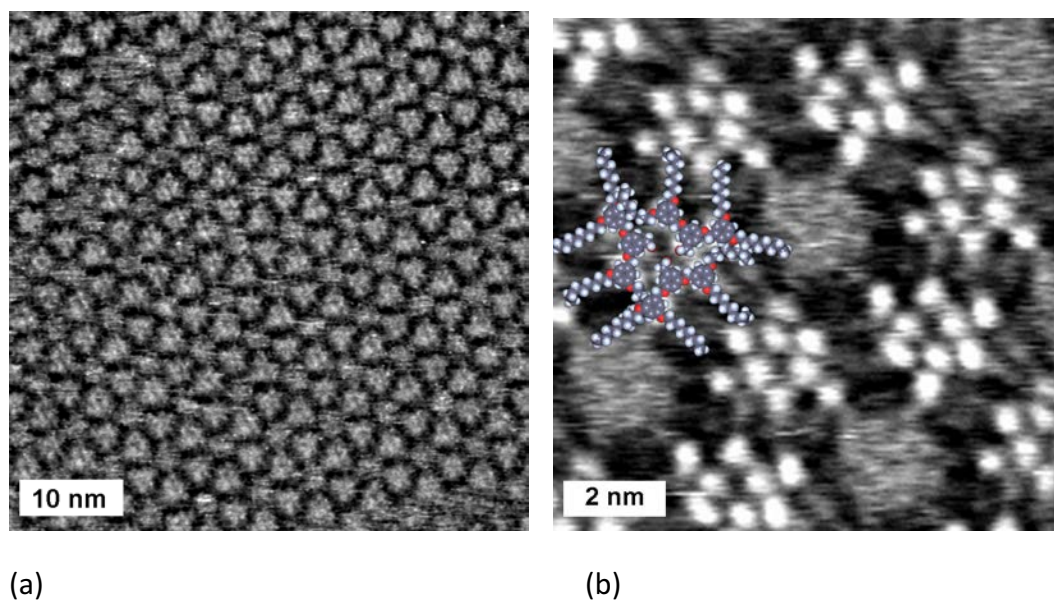


Figure 22 Trimeric assembly of three molecules of the alcohol **8** (a) in an HOPG monolayer of the compound and (b) the molecular fitting (133).

In these later studies we investigated the relationship between the three-dimensional crystal structure of the molecules under investigation and the molecular level organization in the monolayer (136). In some cases there was a very good correlation between the solid state structure and the surface monolayer, but this was not a general phenomenon. In the monolayer the surface-monolayer and intermolecular supramolecular interactions are balanced, whereas in the crystal structure only the intermolecular interactions are relevant. If the surface-monolayer are larger than the

sum of the intermolecular interactions in the monolayer, then the organization will be different. In the solid state, the tpy derivative **9** forms sheets of molecules with interdigitated octyloxy groups (Figure 23a), this same structure is replicated exactly in the monolayer of **9** on HOPG.

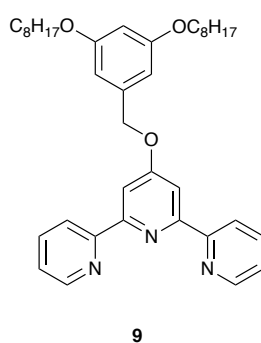
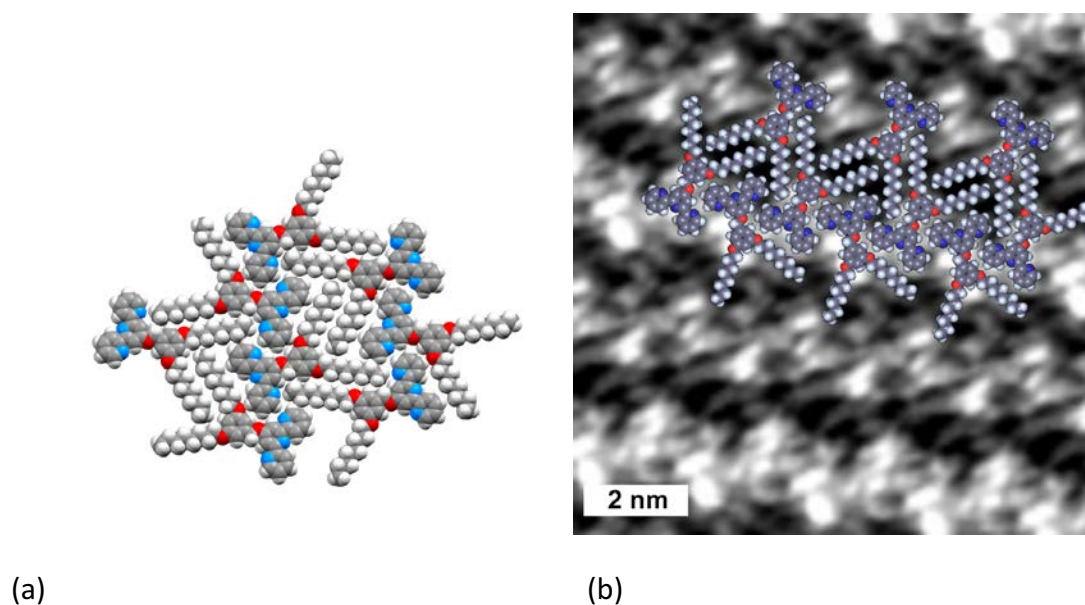


Figure 23 Compound **9** forms sheets of interdigitated molecules in (a) the crystal structure and the same structure is observed (b) in an HOPG monolayer showing the molecular fitting (133).

We had hoped to initiate structural rearrangements in monolayers of functionalized oligopyridines on HOPG by post-treatment with metal salts. In general, this approach

has not been overly successful, mainly because we had underestimated the magnitude of the surface-monolayer interactions. Nevertheless, the monolayers can act as host structures for supramolecular guests. A typical example is seen in Figure 24, in which a monolayer of **8** on HOPG acts as a host to ad-molecules of $[\text{Fe}(\mathbf{10})_2]^{2+}$ (*133*).

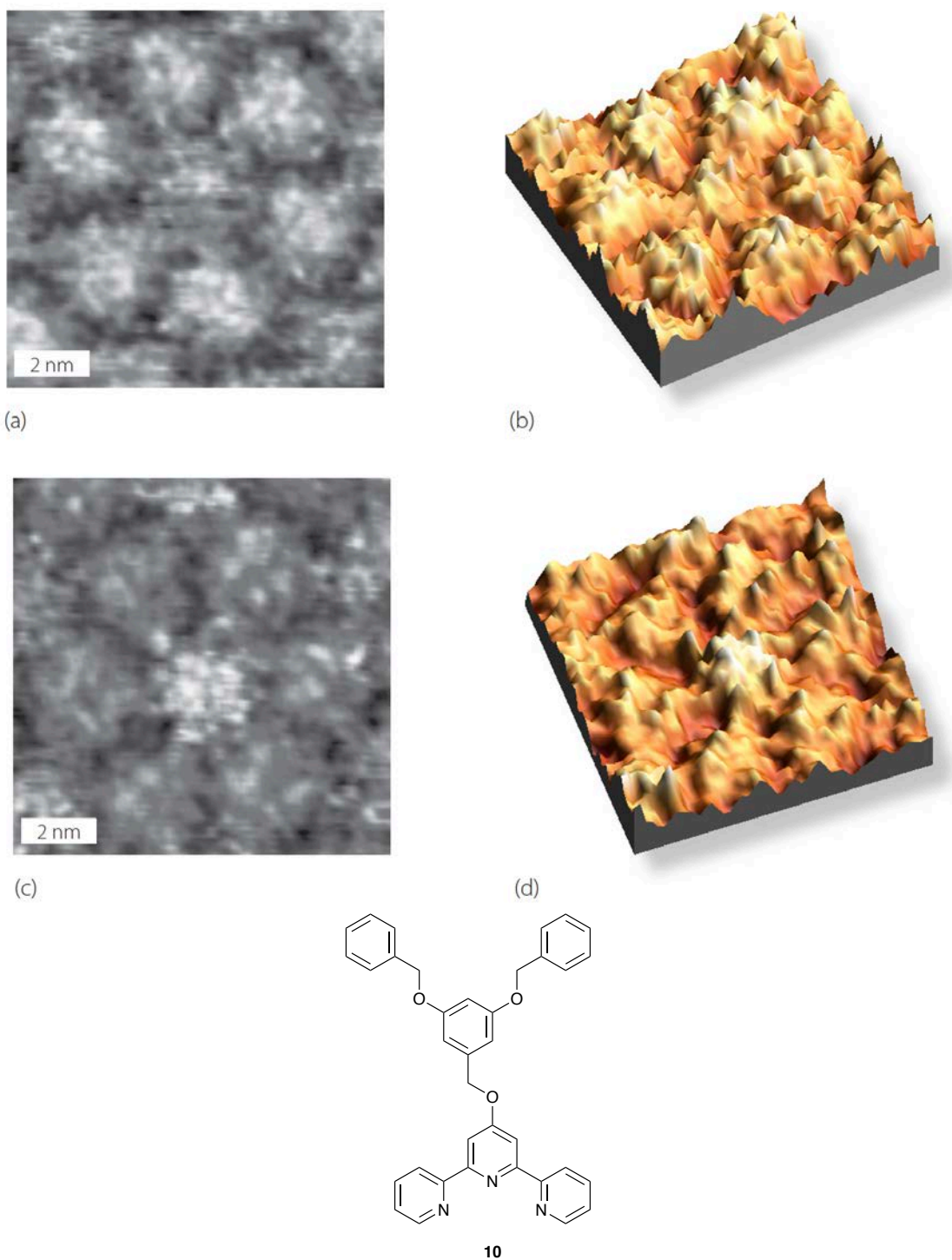
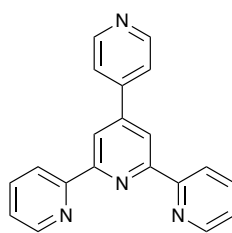


Figure 24 A monolayer of **8** (a) and (b) on HOPG acts as a host to ad-molecules of $[\text{Fe}(\mathbf{10})_2]^{2+}$ (c) and (d) (133).

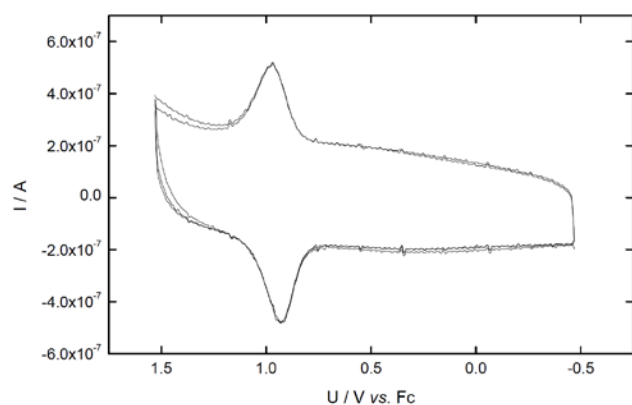
3.3 Combining self-assembly and metallosupramolecular chemistry at surfaces

Is it possible to combine surface supramolecular chemistry with metallosupramolecular chemistry? It was not by accident that many of the compounds we investigated for supramolecular assembly of two dimensional structures at surfaces also contained metal-binding domains, and we had originally conceived this work with the intention of either triggering the restructuring of a monolayer through interaction with metal centres or the forcing of metal centres into unnatural environments through interaction with metal-binding domains constrained to a surface pattern.

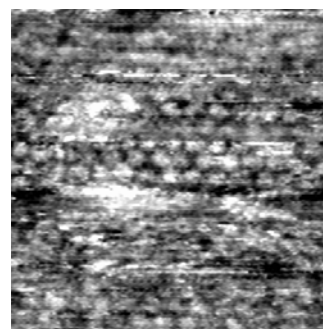
In this short section, we make the transition between supramolecular interactions with surfaces to binding of molecules to the surface (141). We designed the two complexes $[\text{Ru}(\text{tpy})(\mathbf{11})]^{2+}$ and $[\text{Os}(\text{tpy})(\mathbf{11})]^{2+}$ to interact with a noble metal surface through coordination to the pendant pyridine donor of **11**. The complexes form monolayers on platinum microelectrodes which may be interrogated through cyclic voltammetry. This establishes the electronic communication between the adsorbed monolayer and the substrate. Parallel STM studies of a monolayer of $[\text{Ru}(\text{tpy})(\mathbf{11})]^{2+}$ on Pt(100) revealed a close-packed array of the complexes. With this observation, we move to the next stage of this journey.



11



(a)



(b)

Figure 25 The complex $[\text{Ru}(\text{tpy})(\mathbf{11})]^{2+}$ forms monolayers on platinum microelectrodes which exhibit (a) a typical ruthenium(II)-(III) redox response in the cyclic voltammogram and (b) a 45 nm x 45 nm STM image of a monolayer of $[\text{Ru}(\text{tpy})(\mathbf{11})]^{2+}$ on Pt(100) (142).

3.4 From self-assembly to covalent attachment

In this section we complete the transition from solution phase self-assembly and supramolecular self-assembly at surfaces to binding of a complex to a surface through covalent interaction with a substituent on a ligand.

3.4.1 Surface and anchoring algorithms – the new toolkit

Our long-term aim is to develop a versatile tool-kit for the conjugation and optimization of the communication between surfaces and functional molecules. The surfaces that we are particularly interested in are noble metals such as platinum and gold, semiconducting oxides such as TiO₂, fluorine-doped tin oxide (FTO), indium tin oxide (ITO), ZnO or NiO, or other semiconducting chalcogenides such as CdS, CdSe and ZnS. An overview of some of the anchoring groups which comprise the tool-kit for anchoring functional molecules to surfaces is presented in Figure 26.

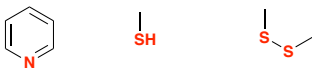
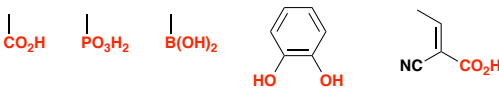
Surface	Anchoring group
Noble metal	
Metal oxide	
Metal sulfide and chalcogenide	

Figure 26 The toolkit of anchoring groups and the surfaces for which they are optimized.

3.5 Taking metallocsupramolecular chemistry to surfaces

3.5.1 The dye-sensitized solar cell

The dye-sensitized solar cell (DSC, also known as the Grätzel cell) converts solar photons to electrical energy using a transparent semiconductor (usually TiO_2) sensitized with with a surface-bound dye that absorbs in the visible region of the spectrum (*143,144,145*) and a representation of a DSC is shown in Figure 27. The dye must have a ground state below and an excited state above the conduction band of the semiconductor and by using surfaces derived from semiconductor nanoparticles, an enormous surface area is achieved in a device with a small surface area. The electrons are harvested at an optically transparent semiconductor electrode and the circuit is completed by an electrolyte hole transporter coupled to a platinized counter-electrode. State of the art dyes for DSCs are based on ruthenium(II) complexes or organic dyes anchored to the surface. The structural features which optimize performance are relatively well understood (*146*). An important non-electronic factor is that aggregation phenomena of dyes at the surface should be minimised.

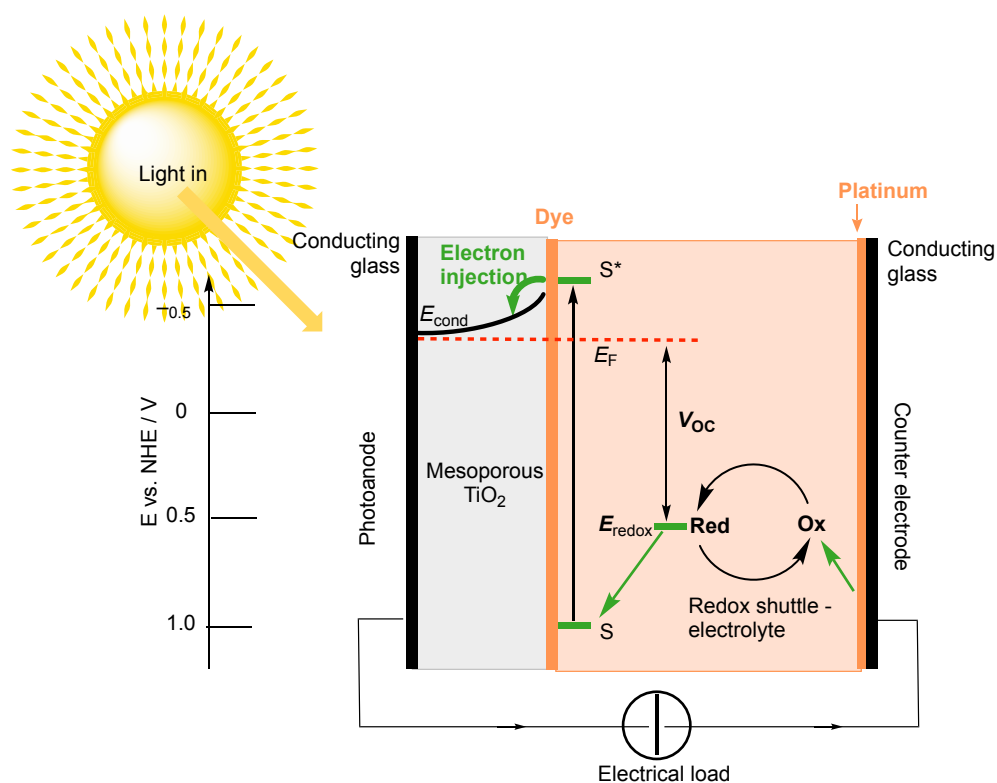


Figure 27 A schematic representation of an n-type dye-sensitized solar cell.

Our recent interests have centred upon the replacement of non-sustainable components in the DSC with materials based upon Earth abundant elements. One approach has been to develop low technology methods for devices using iron oxide and other first row transition metal oxide materials as photoconductors (147,148,149,150,151,152,153,154,155,156) but the main relevance to this review comes in our attempts to replace ruthenium sensitizers in DSCs by Earth abundant metals (157), in particular copper (158).

3.5.2 Copper DSCs

Ruthenium, which is one of the rarest and most expensive elements in the periodic table (abundance 0.000037 ppm in the Earth's crust, US \$ 2090 per kilogram 14th July 2017). Copper is both more abundant (abundance 27 ppm) and cheaper (US \$ 5.9 per kilogram, 14th July 2017). Copper(I) oligopyridine complexes have photophysical properties that resemble those of ruthenium(II) diimine complexes (*159,160*); both $[\text{RuL}_3]^{2+}$ and $[\text{CuL}_2]^+$ complexes (L = bpy or phen ligand) have absorption spectra with maxima 400 - 550 nm, although the absorption coefficient of the Cu species complexes are typically lower than the Ru complexes. In both cases, the excited states are primarily MLCT, although the MLCT state has different character. Excited states of the copper complexes undergo Jahn–Teller distortion with a concomitant flattening of the MLCT leading to enhanced solvent interactions with consequent shortening of the excited state lifetime. We reported some early comparisons of the photophysical properties of copper(I) and ruthenium(II) complexes with ligands optimized for binding copper(I) (*161*). In contrast, the excited and ground state geometries in the ruthenium(II) complexes are very similar resulting in generally longer excited state lifetimes.

With this background it was very surprising that there had been little systematic interest in copper(I) sensitizers for DSCs, with only two reports (*162,163*) appearing before our studies began in 2008 (*164*). One of the reasons for this was the perception among inorganic chemists that copper(I) was labile and, thus, could not be bound in a stable manner to the semiconductor surface in the DSC. Indeed, it was partly the search for non-labile copper(I) complexes that lead Sauvage on the path to the catenates, in which mechanically interlocked systems ensured that ligands could not be exchanged.

We were pleasantly surprised that DSCs sensitized with the complexes $\{\text{Cu}(\mathbf{12})_2\}$ and $\{\text{Cu}(\mathbf{13})_2\}$ (the imprecise formulation relates to the uncertainty regarding the protonation state of the ligands in the dye bath) exhibited high efficiencies of 1.9 – 2.4 % with respect to that of 9.7% for the ruthenium dye N719 (164,165). We have extensively reviewed the development of DSCs using Earth abundant metals, in particular copper, and the reader is referred to these articles for more detailed discussion and the developments outside our own group. (157,158). In this review, we will follow through the development of these prototype systems into a more general assembly algorithm.

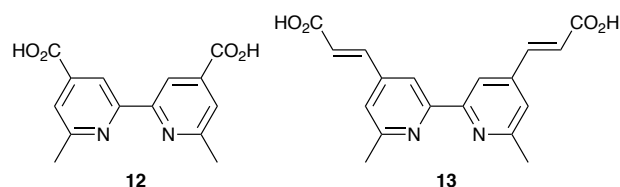


Figure 28 The prototype ligands used for the preparation of copper(I) DSCs

These observations were both encouraging and somewhat perplexing. Encouraging because the cells were relatively efficient, were reasonably long-lived (more on this later), simple ligand design principles worked, and the extended conjugation in complexes of **13** giving a better spectral response. Perplexing because we had expected the cells to be short lived through reaction of copper(I) with the iodide-triiodide electrolyte to generate CuI. The preparation of the cells is presented

schematically in Figure 29 in which the anchor symbol represents the anchoring group, in this case carboxylic acid or carboxylate. We accordingly set about investigating the preparation and optimization of copper-based DSCs in detail.

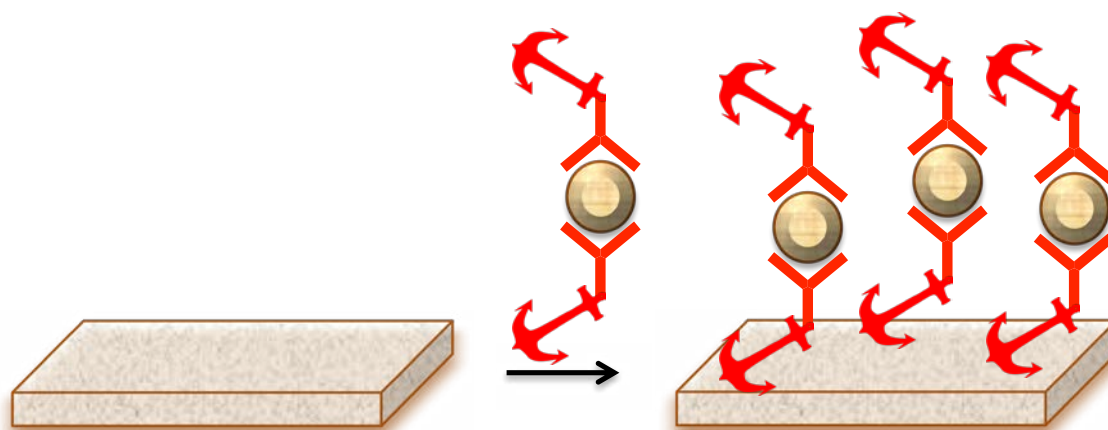
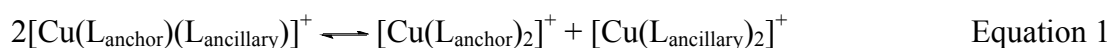


Figure 29 The initial approach adopted for the preparation of copper(I) DSCs. The nanostructured TiO_2 surface was functionalized by reaction with $\{\text{Cu}(\mathbf{12})_2\}$ and $\{\text{Cu}(\mathbf{13})_2\}$ which bound to the surface through one or more carboxylate groups. Although not explicitly depicted, it is also possible that both ligands are surface bound. The anchor symbol represents the anchoring group, in this case carboxylic acid or carboxylate.

We commenced by confirming the lability of copper(I) complexes. Although much of Sauvage's elegant work using copper(I) centres to place molecular threads through macrocycles, we were able to find little quantitative data about ligand exchange rates in copper(I) complexes. In part this reflects the fact that such classical kinetic studies had been performed in aqueous or mixed aqueous solvents, exactly the conditions in which copper(I) disproportionates to copper(0) and copper(II). We recorded the ^1H NMR spectrum of a 1:1 mixture of $[\text{Cu}(6,6'\text{-Me}_2\text{bpy})_2]^+$ (which exhibits one methyl

resonance) and of $[\text{Cu}(\text{2,9-Me}_2\text{phen})_2]^+$ (which also exhibits only one methyl resonance) immediately after mixing (166). The spectrum of the mixture exhibits methyl signals due to the starting homoleptic complexes and due to the 6,6'-Me₂bpy and 2,9-Me₂phen ligands respectively in the heteroleptic complex $[\text{Cu}(6,6'\text{-Me}_2\text{bpy})(\text{2,9-Me}_2\text{phen})]^+$ (Figure 30a). A statistical mixture with 1:1:2 ratios of the two homoleptic and the heteroleptic complex is established. The ¹H exchange spectrum shows clear exchange peaks between the two signals for the 2,9-Me₂phen ligands in the homoleptic and heteroleptic complexes only consistent with fast exchange on the NMR timescale (Figure 30b). We conclude by noting that it is not possible to isolate the heteroleptic complexes with simple ligands of the type illustrated here, but by using ligands with sterically demanding substituents the heteroleptic complexes may be isolated as the major or only products. This is illustrated with bulky substituents in the HETPHEN approach to the design of copper(I) dyes for DSCs (167,168,169,170,171,172) and with macrocyclic ligands incorporating phen metal-binding domains in the work of Sauvage. In our work, this precludes the direct binding of complexes $[\text{Cu}(\text{L}_{\text{anchor}})(\text{L}_{\text{ancillary}})]^+$ (L_{anchor} is the anchoring ligand and $\text{L}_{\text{ancillary}}$ the second ligand attached to the copper(I) centre) to the surface because in solution a mixture of homoleptic and heteroleptic complexes according to equation 1 will be present.



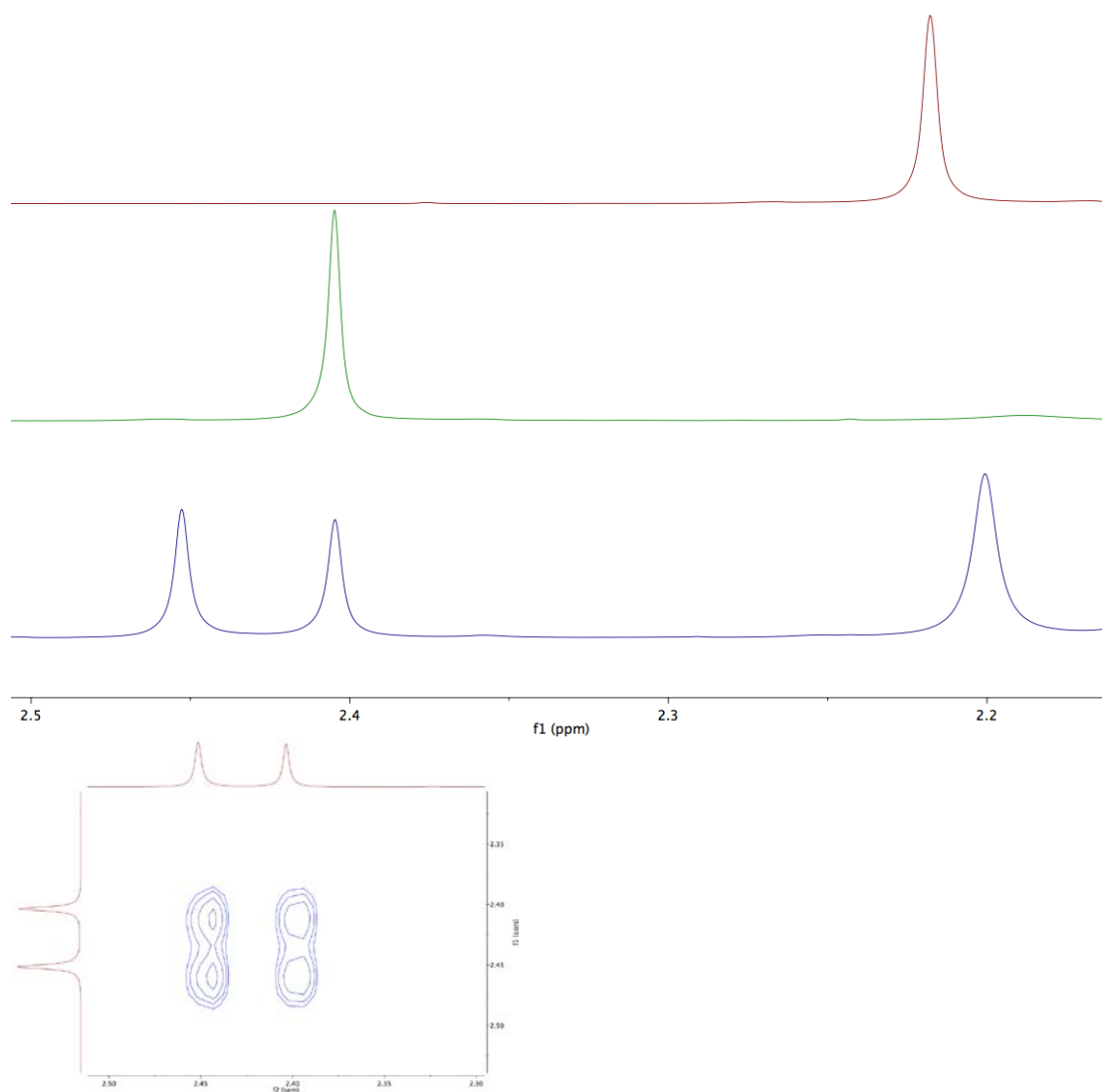


Figure 30 a) The partial 400 MHz ^1H NMR spectra of CD_3CN solutions of $[\text{Cu}(6,6'\text{-Me}_2\text{bpy})_2][\text{PF}_6]$ (top), $[\text{Cu}(2,9\text{-Me}_2\text{phen})_2][\text{PF}_6]$ (middle) and a 1:1 mixture of the two compounds (bottom) showing the methyl region. All solutions were 17 mmol in copper. In the mixture, the methyl signals of the 6,6'- Me_2bpy ligand in the homoleptic and heteroleptic complexes are observed at δ 2.20 ppm, whilst the methyl groups of the 2,9- Me_2phen ligand give signals at δ 2.40 ppm for the homoleptic and δ 2.45 ppm for the heteroleptic complexes. The ^1H NMR exchange

spectrum shows clear exchange peaks between the methyl groups of the Me₂phen ligands in the homoleptic and heteroleptic complexes. (Spectra: Sarah Keller, 2017).

In the course of these studies we developed scanning electrochemical microscopic (SECM) methods to directly interrogate copper(I) DSCs under irradiation and in the dark (173,174). This allowed us access to a powerful method for the high throughput evaluation of combinations of anchoring ligand, ancillary ligand (see later) and electrolyte.

One of the first variables that we sought to optimize was the electrolyte. We had a preconception that the iodide-triiodide electrolyte commonly used in ruthenium DSCs would not be optimal for copper DSCs. In practice, the reaction of iodide with copper(I) does not appear to be a major degradative pathway for copper DSCs. By changing the constitution of the electrolyte and by including additives, the performance can be improved (175). The performances of the copper(I) DSCs was investigated systematically varying the standard electrolyte (LiI, 0.1 M; I₂, 0.05 M; 1-butyl-3-methylimidazolium iodide, 0.6 M; 1-methylimidazole, 0.5 M in 3-methoxypropionitrile. The highest short-circuit current densities and photoconversion efficiencies were obtained with an electrolyte composition I₂ (0.03 M), 1-butyl-3-methylimidazolium iodide (0.6 M), 4-*tert*-butylpyridine (0.4 M) and guanidinium thiocyanate (0.1 M) and no LiI was added. In general, lower concentrations of I₂ are better. The additive guanidinium thiocyanate has no great effect on the performance, and higher concentrations of 4-*tert*-butylpyridine decrease performance. The additives reduce recombination rates at the TiO₂-dye interface.

In an early study, we argued that we could optimize electron transfer to the electrolyte by using an electrolyte as similar as possible to the dye and used the SECM to investigate the use of homoleptic $[\text{Cu}(\text{L}_{\text{ancillary}})_2]^+$ complexes as the electrolyte combined with series of $[\text{Cu}(\text{L}_{\text{anchor}})(\text{L}_{\text{ancillary}})]^+$ dyes. This allowed us to use changes in the diffusion layer at the scanning electrode to map the substrate surface both in the dark and under irradiation. These studies revealed the formation of stable surface charge as the components equilibrate. Nevertheless, the efficiencies of these systems were very low. More successful was the replacement of the iodide-triiodide electrolyte by those based upon $[\text{Co}(\text{bpy})_3]^{2+/3+}$ or $[\text{Co}(\text{phen})_3]^{2+/3+}$ redox couples (176,177). We have made extensive use of electrical impedance spectroscopy (EIS) to study these systems in detail. The photoconversion efficiency is improved by replacing the I_3^-/I^- electrolyte with the cobalt electrolyte and by changing the solvent from MeCN to 3-methoxypropionitrile. The cobalt electrolytes are superior in terms of open-circuit voltage, the short-circuit current and the overall efficiency as a result of faster charge transfer and a more positive redox potential. EIS showed that DSCs with I_3^-/I^- have the highest recombination resistance. There were some differences between $[\text{Co}(\text{bpy})_3]^{2+/3+}$ and $[\text{Co}(\text{phen})_3]^{2+/3+}$ with the phen system giving the highest chemical capacitance, open-circuit voltage and highest mass transport restrictions.

3.6 From "complexes as metals/complexes as ligands" to "surfaces as ligands, surfaces as complexes"

During the last decade of the last Century, a series of fascinating publications from groups in Bologna, Pisa and Messina developed a new strategy for the design and

synthesis of photoactive metallodendrimers for photoharvesting applications. This approach was described as the "complexes as metals, complexes as ligands" strategy and was designed to allow the synthesis of metallodendrimers with defined vectorial electronic and energy transfer properties (178). This strategy had an influence on our way of thinking about ligands and complexes as polyvalent species. This in turn influenced our strategy for the preparation of heteroleptic complexes on surfaces. The strategy presented in Figure 29 is very successful but has three significant disadvantages. The first disadvantage is that systematic variation of the electronic and photophysical properties is not simple and involves the design of a new anchoring ligand in each case. The second disadvantage is that it is not possible to engineer a gradient into the compound, favouring the injection of the electron into the conduction band on the "anchored side" and the stabilization of the hole on the "electrolyte side" of the complex. The final disadvantage is that one of the two ligands bound to the copper centre is, essentially, wasted. These considerations led us to think again about heteroleptic complexes. As discussed above, we ideally required heteroleptic $[\text{Cu}(\text{L}_{\text{anchor}})(\text{L}_{\text{ancillary}})]^+$ complexes which cannot be isolated as discrete species with our simple ligands. The challenge was to find ligands which would either drive the equilibrium in solution to the heteroleptic species, as in the HETPHEN approach, or to find a way to remove the heteroleptic species from the equilibrium. Our early experience with macrocyclic chemistry also shaped our thinking here, as these describe exactly the conditions of the thermodynamic and kinetic template effects (179,180).

Combining all of these factors, we developed the vision of a surface that could act as a ligand and/or as a complex. The key step was to bind the anchoring ligand to the surface as a first step, giving a “surface as ligand” (Figure 31) (166,181).

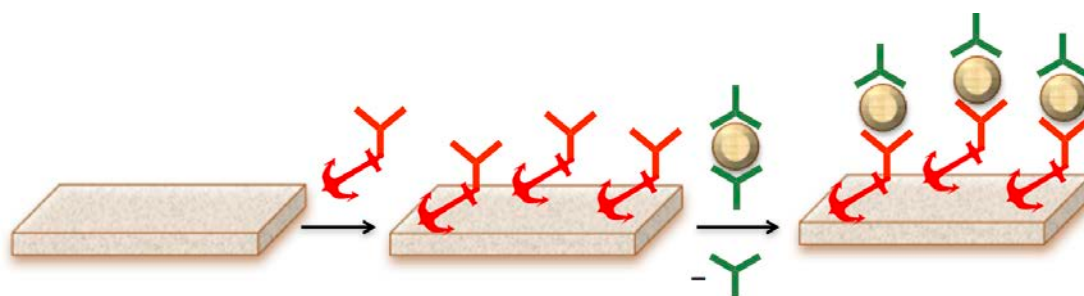


Figure 31 The first “surfaces as ligands, surfaces as complexes” approach. The anchoring ligand is first bound to the semiconductor and a subsequent ligand exchange delivers the $\{\text{Cu}(\text{L}_{\text{ancillary}})\}$ unit to generate the surface bound $\{\text{Cu}(\text{L}_{\text{anchor}})(\text{L}_{\text{ancillary}})\}$ species.

3.6.1 Sequential assembly of copper DSCs – the library of anchors

To implement the “surfaces as ligands, surfaces as complexes” strategy we also developed a suite of anchoring ligands (Figure 32) to complement **12** and **13**, including **14** (182), **15** (182, 183), **16** (165), **17** (174,182,183, 184, 185), **18** (174,175,176,177,181,184,185,186,187,188,189,190,191,192,193,194,195,196,197), **19** (193,198), **20** (191), **21** (191), **22** (192), **23** (192), **24** (192) and **25** (192). In general, anchoring ligands with extended conjugation or aromatic spacers between the anchor and the metal-binding domain perform better in DSCs. A general observation, which we have discussed in detail elsewhere, is that the copper(I) DSCs show an increase in efficiency and performance over a ripening period of up to seven days.

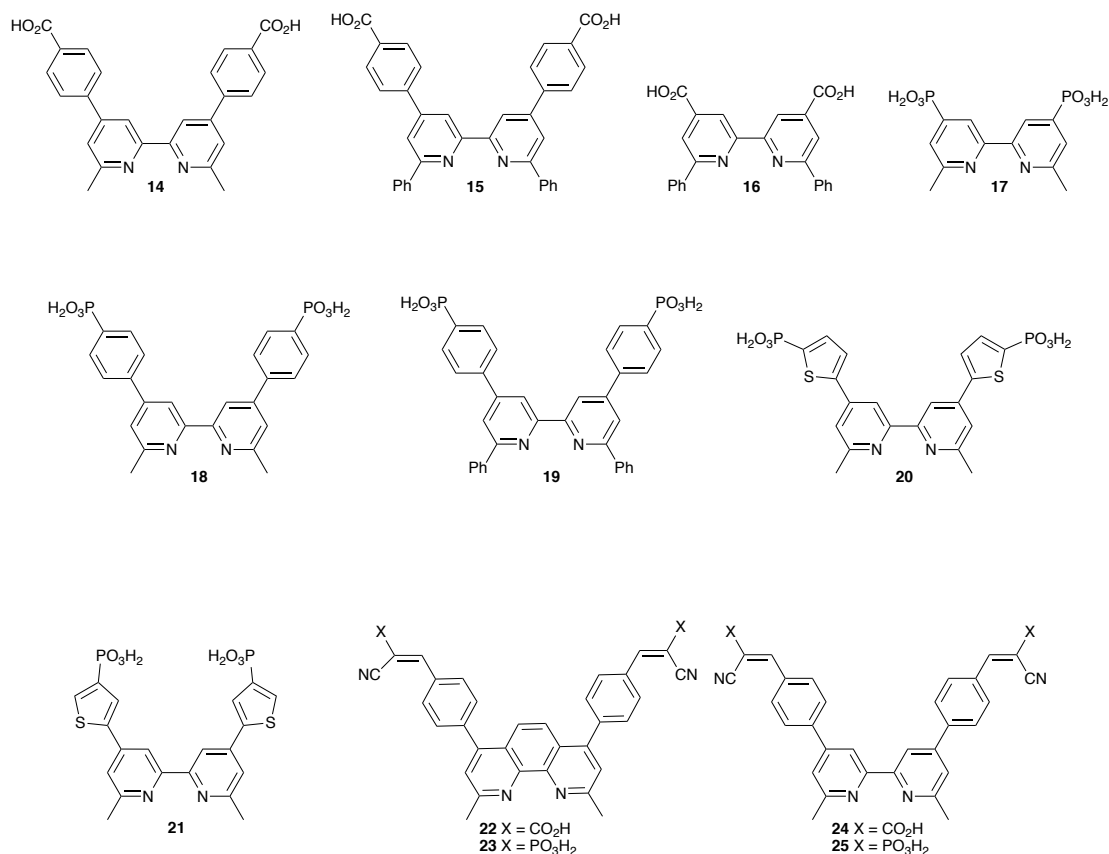
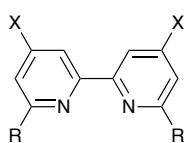


Figure 32 The suite of anchors developed for the “surfaces as ligands, surfaces as complexes” approach. Anchoring groups include carboxylic acids, phosphonic acids, cyanoacrylic acids and α -cyanophosphonic acids.

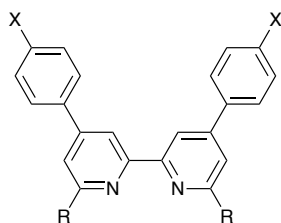
3.6.2 Sequential assembly of copper DSCs – the library of ancillary ligands

The “surfaces as ligands, surfaces as complexes” strategy worked exactly as anticipated, and with this approach we were now able to systematically investigate the variation of $L_{\text{ancillary}}$ in surface bound $[\text{Cu}(L_{\text{anchor}})(L_{\text{ancillary}})]^+$ complexes. We have reviewed these results in detail elsewhere (158). Using the combinatorial approach, we have been able to match the library of anchoring ligands in Figure 32 with a large range of simple ancillary ligands (Figure 33). We have generally adopted 6,6'-

Me₂bpy (**26**) as our reference ancillary ligand (*182*), but we have systematically investigated the effect of the alkyl substituents at the 6,6'-positions by SECM in the series of surface-bound complexes [Cu(L_{anchor})(L_{ancillary})]⁺ (L_{anchor} = **17**, **18**; L_{ancillary} = **27** – **30**) (*174*). DSCs with the series of complexes bound complexes [Cu(L_{anchor})(L_{ancillary})]⁺ (L_{anchor} = **17**, **18**; L_{ancillary} = **27** – **31**) showed optimum performances with ligand **18** and **29** or **31** as the ancillary ligand (*185,198*). Somewhat unexpectedly, very simple ancillary ligands such as **27**, **32**, **33** and **34** perform remarkably well, with the best performances being associated with **34**. We believe that this is due to efficient hole transport to the iodide-triiodide electrolyte (*187,188,193*). Even more surprisingly, surface-bound [Cu(**18**)(**35**)]⁺ with trifluoromethyl substituents in the 6,6'-positions of the ancillary ligand performed exceptionally well (holding the record in our group for a short period) (*194*). The origin of this effect is a little obscure, although DFT calculations confirm the stabilization of the HOMO by the CF₃ substituents, consistent with the performance increase being associated with better *J*_{SC} values.



- 26** R = Me, X = H
35 R = CF₃, X = H



- | | | | |
|-----------|-------------------------------|-----------|----------------|
| 27 | R = Me, X = Br | 32 | R = Me, X = F |
| 28 | R = ⁿ Bu, X = Br | 33 | R = Me, X = Cl |
| 29 | R = ^{iso} Bu, X = Br | 34 | R = Me, X = I |
| 30 | R = ⁿ Hex, X = Br | | |
| 31 | R = Ph, X = Br | | |

Figure 33 Some “simple” ancillary ligands that have been investigated in DSCs with surface-bound $[\text{Cu}(\text{L}_{\text{anchor}})(\text{L}_{\text{ancillary}})]^+$ complexes by the “surfaces as ligands, surfaces as complexes” approach.

Before closing this section, we will consider two additional classes of ancillary ligand. In the course of our work, we often found ourselves asking if it was necessary to have symmetrical ligands or indeed to have substituents in both the 6- and 6'-positions of the bpy. Over the years, we have investigated a series of asymmetric ligands (Figure 34) and in general, there is no significant advantage and the performance is usually inferior to symmetrical analogues (184,189,190,193,194). The exceptions are the trifluoromethyl ancillary ligand **37** which gives very efficient DSCs (194,189).

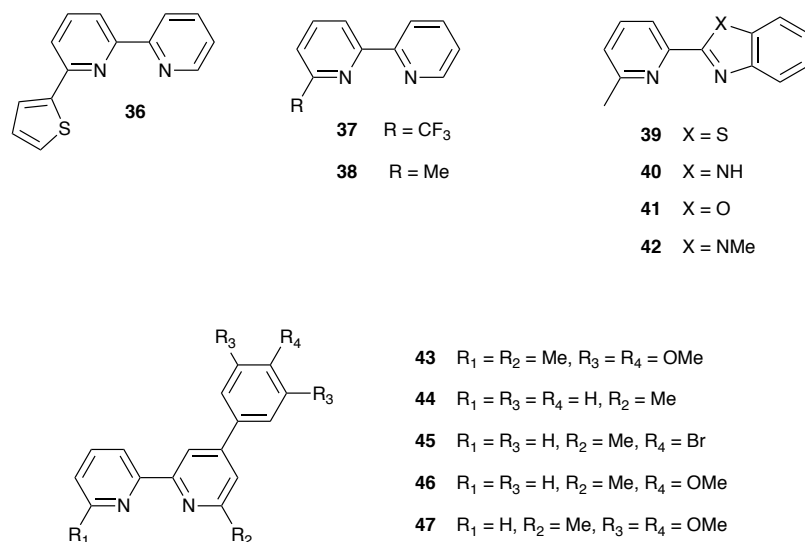


Figure 34 Some asymmetric ancillary ligands that have been investigated in DSCs with surface-bound $[\text{Cu}(\text{L}_{\text{anchor}})(\text{L}_{\text{ancillary}})]^+$ complexes by the “surfaces as ligands, surfaces as complexes” approach.

One final class of ligand is worth mentioning. We have systematically investigated the incorporation of hole-transport substituents with the aim of optimizing hole-transfer to the electrolyte using the library of ancillary ligands including triphenylamino substituents (Figure 35) (175,176,177,182,183,186,188,195,196). The expected improvements in performance are often shown, but do not compete with the synthetically less elegant effects with very simple ligands, in particular trifluoromethyl substituents or 4-haloaryl substituents. Nevertheless, the dendritic systems **52–65** gave us insight into solvent effects and the nature of the ripening processes leading to improved performance of the DSCs over a number of days.

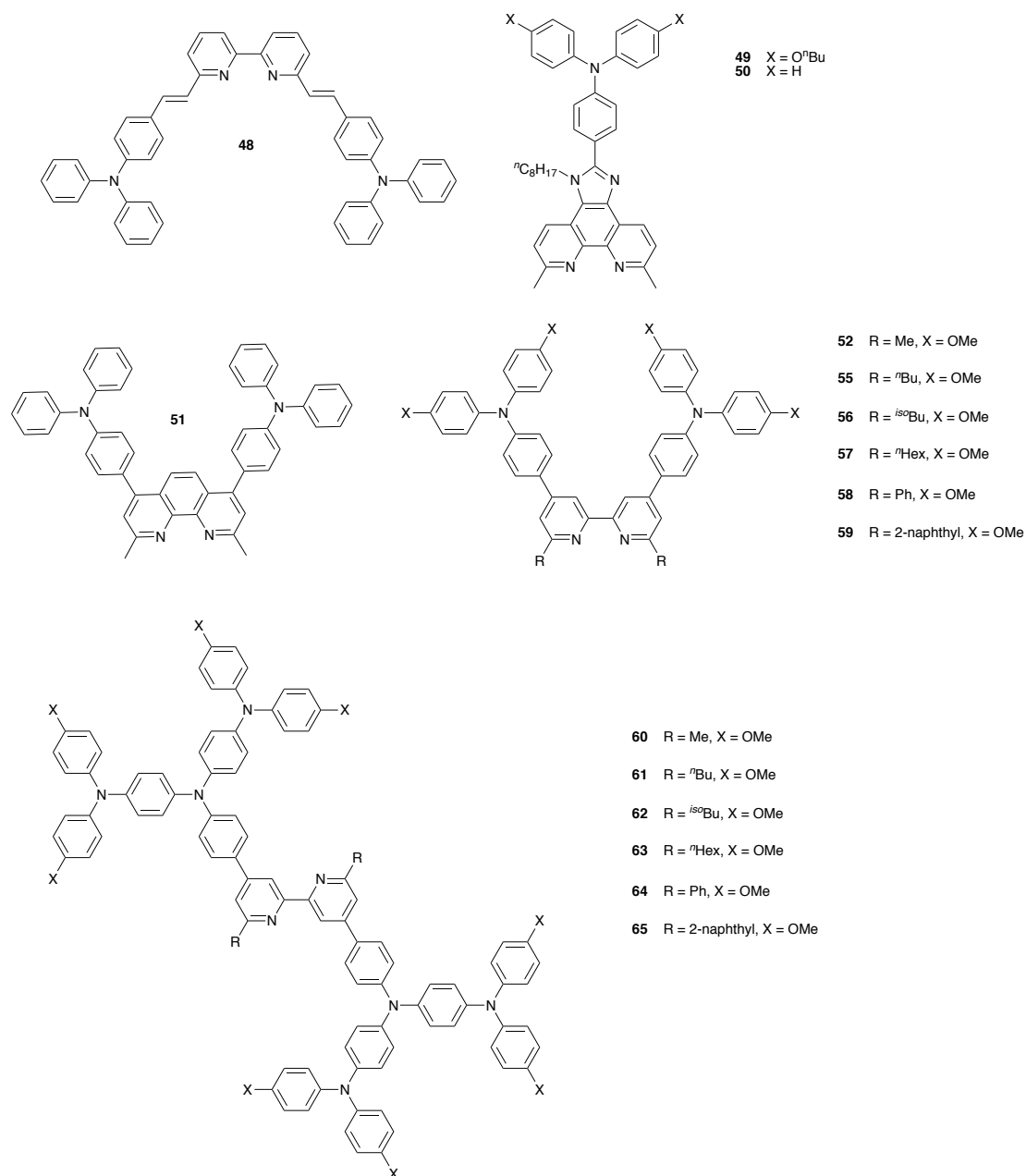


Figure 35 Some hole-transporting ancillary ligands that have been investigated in DSCs with surface-bound $[\text{Cu}(\text{L}_{\text{anchor}})(\text{L}_{\text{ancillary}})]^+$ complexes by the “surfaces as ligands, surfaces as complexes” approach.

3.6.3 Atom economy and regeneration

Inspection of Figure 31 reveals that the use of the exchange reaction between the ligand-functionalized surface and $[\text{Cu}(\text{L}_{\text{ancillary}})_2]^+$ is not optimal in terms of atom economy, as for every new surface-bound complex that is formed, one equivalent of $\text{L}_{\text{ancillary}}$ is wasted. This may be of little consequence with commercially available ligands such as **26**, but for dendritic ancillaries such as **60** – **65**, which involve many tens of man-hours for their synthesis, it is of significant concern. The final refinement of the “surfaces as ligands, surfaces as complexes” approach addresses this issue (Figure 36). In this approach, the ligand-functionalized surface is either reacted with a solution containing a 1:1 mixture of $[\text{Cu}(\text{MeCN})_4]^+$ and the desired ancillary ligand (a formulation equivalent to $[\text{Cu}(\text{L}_{\text{ancillary}})(\text{MeCN})_2]^+$ (Figure 36a) or is sequentially treated with $[\text{Cu}(\text{MeCN})_4]^+$ followed by $\text{L}_{\text{ancillary}}$ (Figure 36b). Both of these approaches are successful (*181,186,188,198*).

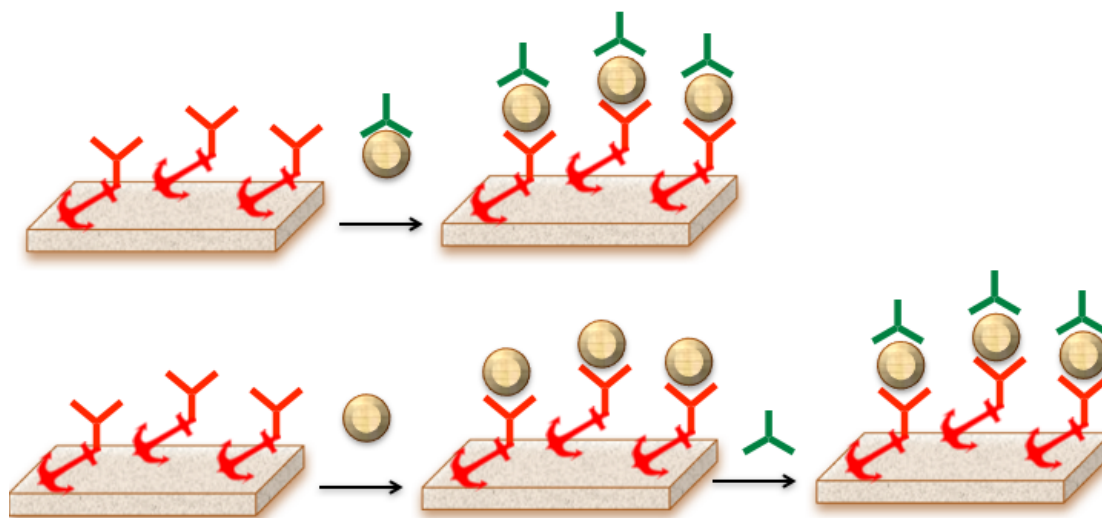


Figure 36 The atom-economical “surfaces as ligands, surfaces as complexes” approach. The anchoring ligand is first bound to the semiconductor and then either (a) reacted with a solution containing a 1:1 mixture of $[\text{Cu}(\text{MeCN})_4]^+$ and $\text{L}_{\text{ancillary}}$ or (b) sequentially reacted with $[\text{Cu}(\text{MeCN})_4]^+$ followed by $\text{L}_{\text{ancillary}}$.

Finally, we note that it is possible to use this strategy to regenerate “dead” DSCs. The bleaching process involves loss of copper(I) and not detachment of the anchoring ligand from the surface (198). We have demonstrated that treatment of a bleached cell sequentially with $[\text{Cu}(\text{MeCN})_4]^+$ followed by $\text{L}_{\text{ancillary}}$ regenerates the surface bound dye (198). Such a regeneration is not possible, to the best of our knowledge, for DSCs utilizing ruthenium dyes.

3.6.4 The future

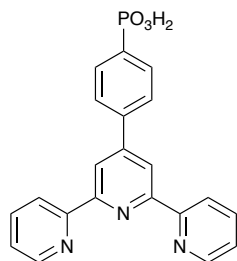
Is this approach limited to copper(I) DSCs? Here again, the first results are extremely optimistic. We have shown that by generating a new library of anchoring ligands **66** and **67** and ancillary ligands **68** – **75** based upon tpy metal-binding domains (Figure 37) the strategy can be extended to octahedral metal centres and we have given proof of concept with zinc(II) surface bound materials. In this case, although the d^{10} zinc(II) centre does not give strong MLCT bands, by using ancillary ligands which absorbed strongly in the visible, it was possible to fabricate functioning DSCs (199,200,201). The strategy used was based upon Figure 36b, in which the surface was first functionalized with the anchor **66** or **67** and subsequently sequentially treated with zinc(II) salts and the ancillary ligand. This indicated a development of the approach in which it should be possible to combine metal-centred and organic dyes for optimal sensitization across the spectrum. This has been demonstrated by the use of the ancillary ligand **75**.

One of the major disadvantages of copper(I) DSCs is that the spectral response is less than with ruthenium-based or organic dyes. Very recently, we have shown that co-sensitization of copper DSCs with the blue organic dye **76** gives robust and sustainable devices with performances beginning to approach state-of-the-art ruthenium dyes; the best performing co-sensitized system achieved an efficiency of 65.6% relative to N719 (189). We consider that the hierarchical approach is ideally suited for the fabrication of panchromatic systems using multiple and complementary chromophores. We recently reported a first approach to functionalization with multiple complexes in the preparation of efficient copper(I) DSCs bearing surface-

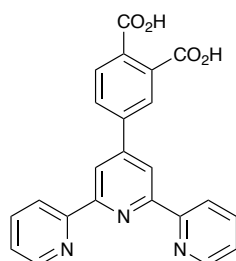
bound $[\text{Cu}(\mathbf{18})(\text{L}_{\text{ancillary}})]^+$ ($\text{L}_{\text{ancillary}} = \mathbf{39}$ and $\mathbf{40}$) (190) and organic dyes in hierarchical assemblies.

The sequential treatment with metal ion followed by ligand opens up a new possibility for the designed assembly of interfacial hierarchical systems. Although one-dimensional coordination polymers are potentially conducting wires for interfacing nanostructured devices, the selective interfacing and orientation with respect to the surface is usually difficult to control. We have recently shown that if the ancillary ligand is ditopic, it can convert a "surface as complex" back to a "surface as ligand" (Figure 38). Consider the ditopic ligand **77** which contains two spatially separated bpy metal-binding domains optimized for copper(I) by the methyl groups at the 6,6'-positions. Sequential treatment of a surface functionalized with **18** (**A**) with $[\text{Cu}(\text{MeCN})_4]^+$ followed by **77** gives the surface-bound complex $[\text{Cu}(\mathbf{18})(\mathbf{77})]^+$, **B**. However, **B** is not only a complex but it is also a ligand by virtue of the uncoordinated bpy metal-binding domain. Subsequent treatment with $[\text{Cu}(\text{MeCN})_4]^+$ followed by **77** gives the surface-bound dinuclear complex $[\text{Cu}(\mathbf{18})(\mathbf{77})\text{Cu}(\mathbf{77})]^{2+}$, **C** which is once again both a complex and a ligand. Further treatment with $[\text{Cu}(\text{MeCN})_4]^+$ followed by **77** gives the surface-bound trinuclear complex $[\text{Cu}(\mathbf{18})(\mathbf{77})\text{Cu}(\mathbf{77})\text{Cu}(\mathbf{77})]^{3+}$, **D** (181). Repeated cycles of treatment with $[\text{Cu}(\text{MeCN})_4]^+$ followed by **77** allows the iterative assembly of the one-dimensional coordination polymer linked to the surface by the anchoring ligand (181). A very subtle change in the ditopic ligand from **77** which has two metal-binding domains optimized for copper(I), to the heteroditopic ligand **78** which possesses a metal-binding domain optimized for copper(I) and one which can bind a $\{\text{Ru}(\text{bpy})_2\}$ moiety

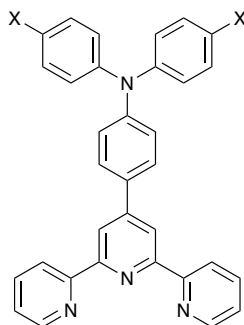
allows the specific and spatially controlled synthesis of heterodinuclear complexes containing two different metal-based chromophores (181).



66

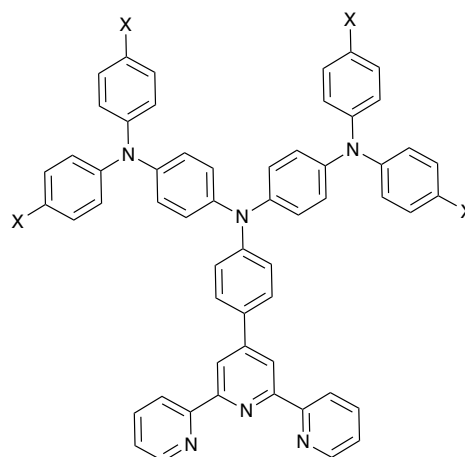


67



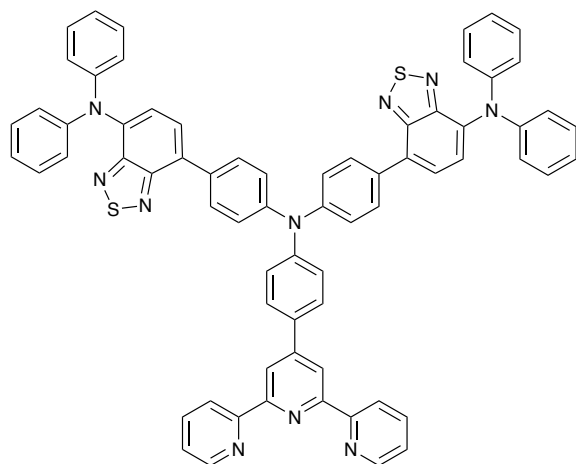
68 X = H

69 X = OMe

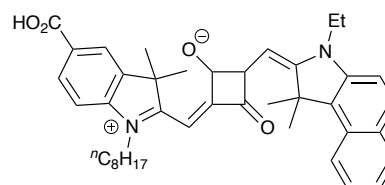
70 X = OⁿBo71 X = O^{iso}Bu72 X = OⁿOct

73 X = H

74 X = OMe



75 X = H



76

Figure 37 The new library of anchoring and ancillary ligands developed for extension of the “surfaces as ligands, surfaces as complexes” approach to octahedral metal centres using tpy metal-binding domains to generate surface-bound $[\text{Zn}(\text{L}_{\text{anchor}})(\text{L}_{\text{ancillary}})]^{2+}$.

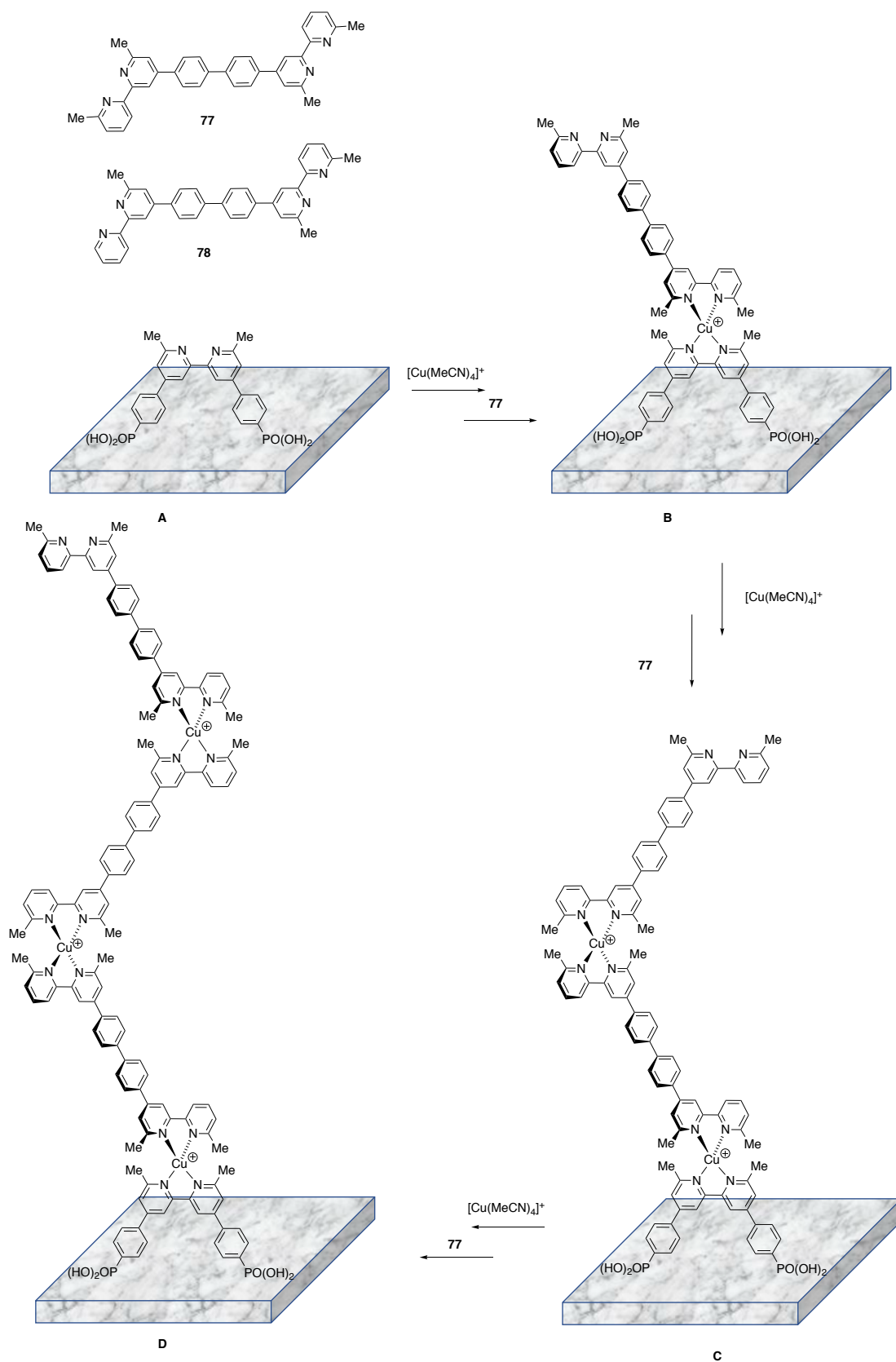


Figure 38 Using ditopic ancillary ligands the “surfaces as ligands, surfaces as complexes” approach allows the specific synthesis of coordination polymers in a controlled and stepwise manner.

4. Acknowledgements

This article has described a journey. It has been a long journey with many interesting excursions and blind alleys and is a journey that has not yet come to its destination. I hope that in some way I have been able to show how various ideas and concepts evolved and transferred from one area of activity to another. As always, the real heroes of this story are the companions who travelled along the same way and I once again take the opportunity to thank the many talented co-workers and colleagues who have made this journey possible, and of course Professor Catherine Housecroft as long-term collaborator in both science and life!

5. References

1. Steed, J.W.; Atwood, J.L.; Gale, P.A. *Supramolecular Chemistry: From Molecules to Nanomaterials*, John Wiley & Sons, Ltd., 2012 DOI: 10.1002/9780470661345.smc002.
2. Halley, J.D.; Winkler, D.A. *Complexity* **2008**, *14*, 10.
3. Anderson, S.; Constable, E.C.; Dare-Edwards, M.P.; Goodenough, J.B.; Hamnett, A.; Seddon, K.R.; Wright, R.D. *Nature* **1979**, *280*, 571.
4. O'Regan, B.; Grätzel, M. *Nature* **1991**, *353*, 737.
5. Hagfeldt, A.; Boschloo, G.; Sun, L.; Kloo, L.; Pettersson, H. *Chem. Rev.* **2010**, *110*, 6595.
6. Grätzel, M. *Acc. Chem. Rev.* **2009**, *42*, 1788.
7. Luman, C.R.; Castellano, F.N. In *Comprehensive Coordination Chemistry, Vol 1*; McCleverty, J.A., Meyer, T.J., Lever, A.B.P., Eds.; Elsevier: Oxford, 2004, p. 25.
8. Kaes, C.; Katz, A.; Hosseini, M.W. *Chem. Rev.* **2000**, *100*, 3553.
9. Sammes, P.G.; Yahioğlu, G. *Chem. Soc. Rev.* **1994**, *23*, 327.
10. Constable, E.C. *Adv. Inorg. Chem.* **1986**, *30*, 69.
11. Schubert, U.S.; Hofmeier, H.; Newkome, G.R. *Modern Terpyridine Chemistry*; Wiley: Weinheim, 2006.
12. Constable, E.C. *Prog. Inorg. Chem.* **1994**, *42*, 67.
13. Schubert, U.S.; Winter, A.; Newkome, G.R. *Terpyridine-based Materials: For Catalytic, Optoelectronic and Life Science Applications*; Wiley: Weinheim, 2011.
14. Constable, E.C. *Chem. Soc. Rev.* **2007**, *36*, 246.
15. Buckingham, A.D., Legon, A.C., Roberts, S.M. Eds. *Principles of Molecular Recognition*; Springer: Dordrecht, 1993.
16. Chatterji, D. *Basics of molecular recognition*; CRC Press, Taylor and Francis Group: Boca Raton, 2016.
17. "The Nobel Prize in Chemistry 1987". *Nobelprize.org*. Nobel Media AB 2014. Web. 6 Jul 2017.
<http://www.nobelprize.org/nobel_prizes/chemistry/laureates/1987/>
18. Lehn, J.-M. *Angew. Chem. Int. Ed. Engl.* **1988**, *27*, 89.
19. Chung, C.-S. *Inorg. Chem.* **1979**, *18*, 1321.
20. Myers, R. T. *Inorg. Chem.* **1978**, *17*, 952.
21. Hancock, R. D.; Martell, A. E. *Comments Inorg. Chem.* **1988**, *6*, 237.
22. Martell, A. E.; Hancock, R. D.; Motekaitis, R. J. *Coord. Chem. Rev.* **1994**, *133*, 39.
23. Lindoy, L.F. *The Chemistry of Macrocyclic Ligand Complexes*; Cambridge University Press: Cambridge, 1990.
24. Pearson, R. G. *Chemical Hardness*; Wiley-VCH Verlag: Weinheim, 1997.
25. Burgess, J.; Tobe, M.L., *Inorganic Reaction Mechanisms*; Pearson: London, 1999.
26. Constable, E.C.; Lewis, J.; Liptrot, M.C.; Raithby, P.R.; Schröder, M. *Polyhedron* **1983**, *2*, 301.

-
27. Constable, E.C.; Lewis, J.; Liptrot, M.C.; Raithby, P.R. *J. Chem. Soc., Dalton Trans.* **1984**, 2177.
 28. Constable, E.C.; Khan, F.K.; Lewis, J.; Liptrot, M.C.; Raithby, P.R.; *J. Chem. Soc., Dalton Trans.* **1985**, 333.
 29. Chung, L.-Y.; Constable, E.C.; Lewis, J.; Raithby, P.R.; Vargas, M.D. *J. Chem. Soc., Chem. Commun.* **1984**, 1425.
 30. Chung, L.-Y.; Constable, E.C.; Dale, A.R.; Khan, M.S.; Liptrot, M.C.; Lewis, J.; Raithby, P.R. *J. Chem. Soc., Dalton Trans.* **1990**, 1397.
 31. Oerpen, G.; Vogtle, F. *Liebigs Ann. Chem.* **1979**, 2114.
 32. Constable, E.C.; Doyle, M.J.; Healy, J.; Raithby, P.R. *J. Chem. Soc., Chem. Commun.* **1988**, 1262.
 33. Constable, E.C. *Chem. Ind.* **1994**, 56-59.
 34. Seddon Ru book
 35. Luis, E.T.; Ball, G.E.; Gilbert, A.; Iranmanesh, H.; Newdick, C.W.; Beves, J.E. *J. Coord. Chem.* **2016**, 69, 1686.
 36. Chotalia, R.; Constable, E.C.; Hannon, M.J.; Tocher, D.A. *J. Chem. Soc., Dalton Trans.* **1995**, 3571.
 37. Constable, E.C.; Cargill Thompson, A.M.W.C. *Inorg. Chim. Acta* **1994**, 223, 177.
 38. Blackman, A.G. *C.R. Chimie* **2005**, 8, 107.
 39. Constable, E.C.; Housecroft, C.E. *Coord. Chem. Rev.* **2017**, in press: <https://doi.org/10.1016/j.ccr.2017.06.006>.
 40. Chan, C.-W.; Che, C.-M.; Cheng, M.-C.; Wang, Y. *Inorg. Chem.*, **1992**, 31, 4874.
 41. Constable, E.C.; Elder, S.M.; Healy, J.; Ward, M.D.; Tocher, D.A. *J. Am. Chem. Soc.* **1990**, 112, 4590.
 42. Constable, E.C.; Elder, S.M.; Hannon, M.J.; Martin, A.; Raithby, P.R.; Tocher, D.A. *J. Chem. Soc., Dalton Trans.* **1996**, 2423.
 43. <https://doi.org/10.1351/goldbook.K03366>
 44. Canty, A.J.; Chaichit, N.; Gatehouse, B.M.; Marker, A. *Acta Crystallogr., Sect. B: Struct. Sci.* **1978**, B34, 3229.
 45. Carroll, L. *Through the Looking-Glass and What Alice Found There*; Macmillan and Co.: London, 1872; <http://www.gutenberg.org/files/12/12-h/12-h.htm>.
 46. Piguet, C.; Bernardinelli, G.; Hopfgartner, G. *Chem. Rev.* **1997**, 97, 2005.
 47. Constable, E.C. *Tetrahedron* **1992**, 48, 10013.
 48. Constable, E. C. In *Comprehensive Supramolecular Chemistry*; Atwood, J. L.; Davies, J. E. D., MacNicol, D. D., Vögtle, F., Eds, Pergamon: Oxford, 1996; p 213. Chapter 6.
 49. Boiocchi, M.; Fabbrizzi, L. *Chem. Soc. Rev.* **2014**, 43, 1835.
 50. Machado, V.G.; Baxter, P.N.W.; Lehn, J.-M. *J. Braz. Chem. Soc.* **2001**, 12, 431.
 51. Constable, E.C.; Hannon, M.J.; Martin, A.; Raithby, P.R.; and D.A. Tocher, *Polyhedron*, **1992**, 11, 2967.
 52. Serr, B.R.; Andersen, K.A.; Elliott, C.M.; Anderson, O.P. *Inorg. Chem.* **1988**, 27, 4499.
 53. Albrecht, M. *Chem. Rev.* **2001**, 101, 3457.
 54. Baum, G.; Constable, E.C.; Fenske, D.; Housecroft, C.E.; Kulke, T. *J. Chem. Soc., Chem. Commun.* **1999**, 195.

-
55. Constable, E.C.; Chotalia, R. *J. Chem. Soc., Chem. Commun.* **1992**, 64.
 56. E. C. Constable, Edwards, A.J.; Martínez-Máñez, R.; Raithby, P.R. *J. Chem. Soc., Dalton Trans.* **1995**, 3253.
 57. Liu, P.; Liu, Y.; Wong, E.L.-M.; Xiang, S.; Che, C.-M. *Chem. Sci.* **2011**, 2, 2187.
 58. Constable, E.C.; Ward, M.D.; Tocher, D.A. *J. Am. Chem. Soc.* **1990**, 112, 1256.
 59. Constable, E.C.; M.D. Ward and D.A. Tocher, *J. Chem. Soc., Dalton Trans.* **1991**, 1675.
 60. Potts, K.T.; Keshavarz-K, M.; Tham, F.S.; Abruna, H.D.; Arana, C. *Inorg. Chem.* **1993**, 32, 4436.
 61. Constable, E.C.; Neuburger, M.; Smith, D.R.; Zehnder, M. *J. Chem. Soc., Chem. Commun.* **1996**, 1917.
 62. Chotalia, R.; Constable, E.C.; Neuburger, M.; Smith, D.R.; Zehnder, M. *J. Chem. Soc., Dalton Trans.* **1996**, 4207.
 63. Chen, M.; Ng, S.-M.; Yiu, S.-M.; Lau, K.C.; Zeng, R.J.; Lau, T.-C. *J. Chem. Soc., Chem. Commun.* **2014**, 50, 14956.
 64. Potts, K.T.; Keshavarz-K, M.; Tham, F.S.; Raiford, K.A.G.; Arana, C.; Abruna, H.D. *Inorg. Chem.* **1993**, 32, 5477.
 65. Potts, K.T.; Wentland, M.P.; Ganguly, D.; Storrier, G.D.; Cha, S.K.; Cha, J.; Abruna, H.D. *Inorg. Chim. Acta* **1999**, 288, 189.
 66. Constable, E.C.; Edwards, A.J.; Hannon, M.J.; Raithby, P.R.; *J. Chem. Soc., Chem. Commun.* **1994**, 1991.
 67. Al-Anber, M.; Walfort, B.; Vatsadze, S.; Lang, H. *Inorg. Chem. Commun.* **2004**, 7, 799.
 68. Potts, K.T.; Keshavarz-K, M.; Tham, F.S.; Abruna, H.D. Arana, C. *Inorg. Chem.* **1993**, 32, 4450.
 69. Constable, E.C.; Kulke, T.; Neuburger, M.; Zehnder, M. *Chem. Commun.* **1997**, 489.
 70. Baum, G.; Constable, E.C.; Fenske, D.; Housecroft, C.E.; Kulke, T. *Chem. Commun.* **1998**, 2659.
 71. Baum, G.; Constable, E.C.; Fenske, D.; Housecroft, C.E.; Kulke, T.; Neuburger, M.; Zehnder, M. *J. Chem. Soc., Dalton Trans.* **2000**, 945.
 72. Yeung, C.-T.; Yeung, H.-L.; Tsang, C.-S.; Wong, W.-Y.; Kwong, H.-L. *Chem. Commun.* **2007**, 5203.
 73. Cui, Y.; He, C. *J. Am. Chem. Soc.* **2003**, 125, 16202.
 74. Marsh, R.E.; Clemente, D.A. *Inorg. Chim. Acta* **2007**, 360, 4017.
 75. Hou, L.; Li, D. *Inorg. Chem. Commun.* **2005**, 8, 128.
 76. Ma, Z.; Xing, Y.; Yang, M.; Hu, M.; Liu, B.; Guedes de Silva, M.F.C.; Pombeiro, A.J.L. *Inorg. Chim. Acta* **2009**, 362, 2921.
 77. Fik, M.A.; Gorczynski, A.; Kubicki, M.; Hnatejko, Z.; Fedoruk-Wyszomirska, A.; Wyszko, E.; Giel-Pietraszuk, M.; Patroniak, V. *Eur. J. Med. Chem.* **2014**, 86, 456.
 78. Constable, E.C.; Drew, M.G.B.; Forsyth, G.; Ward, M.D. *J. Chem. Soc., Chem. Commun.* **1988**, 1450.
 79. Fu, Y.; Li, Q.; Zhou, Z.; Dai, W.; Wang, D.; Mak, T.C.W.; Hu, H.; Tang, W.J. *J. Chem. Soc., Chem. Commun.* **1996**, 1549.
 80. Wong, E.L.-M.; Fang, G.-S.; Che, C.M.; Zhu, N. *J. Chem. Soc., Chem. Commun.* **2005**, 4578.
 81. Liu, P.; Liu, Y.; Wong, E.L.-M.; Xiang, S.; Che, C.-M. *Chem. Sci.* **2011**, 2, 2187.

-
82. Fu, Y.J.; Gao, Z.-S.; Yang, H.; Dai, W.; Wang, D.; Hu, H.; Tang, W.; Zhang, Z.; Mak, T.C.W. *Acta Crystallogr., Sect. C: Cryst. Struct. Commun.* **1999**, *55*, 349.
83. Gheysen, K.A.; Potts, K.T.; Hurrell, H.C.; Abruna, H.D. *Inorg. Chem.* **1990**, *29*, 1589.
84. Marsh, R.E. *Acta Crystallogr., Sect. B: Struct. Sci.* **1997**, *53*, 317.
85. Constable, E.C.; Walker, J.V.; Tocher, D.A.; Daniels, M.A.M. *J. Chem. Soc., Chem. Commun.* **1992**, 768.
86. Constable, E.C.; Daniels, M.A.M.; Drew, M.G.B.; Tocher, D.A.; Walker, J.V.; Wood, P.D. *J. Chem. Soc., Dalton Trans.* **1993**, 1947.
87. Dai, W.; Hu, H.; Wei, X.; Zhu, S.; Wang, D.; Yu, K.; Dalley, N.K.; Kou, X. *Polyhedron* **1997**, *16*, 2059.
88. Ho, P.K.-K.; Cheung, K.-K.; Peng, S.-M.; Che, C.-M. *J. Chem. Soc., Dalton Trans.* **1996**, 1411.
89. Constable, E.C.; Drew, M.G.B.; Ward, M.D. *J. Chem. Soc., Chem. Commun.* **1987**, 1600.
90. Barley, M.; Constable, E.C.; Corr, S.A.; McQueen, R.C.S.; Nutkins, J.C.; Ward, M.D.; Drew, M.G.B. *J. Chem. Soc., Dalton Trans.* **1988**, 2655.
91. Potts, K.T.; Keshavarz-K, M.; Tham, F.S.; Abruna, H.D.; Arana, C. *Inorg. Chem.* **1993**, *32*, 4422.
92. Constable, E.C.; Elder, S.M.; Raithby, P.R.; Ward, M.D. *Polyhedron* **1991**, *10*, 1395.
93. Constable, E.C.; Neuburger, M.; Whall, L.A.; Zehnder, M. *New J. Chem.* **1998**, *22*, 219.
94. Constable, E.C.; Ward, M.D.; Drew, M.G.B.; Forsyth, G.A. *Polyhedron* **1989**, *8*, 2551.
95. Ho, P.K.-K.; Cheung, K.-K.; Che, C.-M. *J. Chem. Soc., Chem. Commun.* **1996**, 1197.
96. Constable, E.C.; Figgemeier, E.; Hougén, I.A.; Housecroft, C.E.; Neuburger, M.; Schaffner, S.; Whall, L.A. *J. Chem. Soc., Dalton Trans* **2005**, 1168.
97. Chaurin, V.; Constable, E.C.; Housecroft, C.E. *New J. Chem.* **2006**, *30*, 1740.
98. Fu, Y.; Sun, J.; Li, Q.; Chen, Y.; Dai, W.; Wang, D.; Mak, T.C.W.; Tang, W.; Hu, H. *J. Chem. Soc., Dalton Trans.* **1996**, 2309.
99. Aguado, J.E.; Calhorda, M.J.; Costa, P.J.; Crespo, O.; Felix, V.; Gimeno, M.C.; Jones, P.G.; Laguna, A. *Eur. J. Inorg. Chem.* **2004**, 3038.
100. Constable, E.C.; A.J. Edwards, Raithby, P.R.; J.V. Walker *Angew. Chem., Int. Ed. Engl.* **1993**, *32*, 1465.
101. Constable, E.C.; Edwards, A.J.; Raithby, P.R.; Smith, D.R.; Walker, J.V.; Whall, L.A. *J. Chem. Soc., Chem. Commun.* **1996**, 2551.
102. Lam, K.S.; Lebl, M.; Krcn'ák, V. *Chem. Rev.* **1997**, *97*, 411
103. Jung, G. Ed. *Combinatorial Chemistry: Synthesis, Analysis, Screening*; Wiley: Weinheim, 2008.
104. Corbett, P.T.; Leclaire, J.; Vial, L.; West, K. R.; Wietor, J.-L.; Sanders, J.K.M.; Otto, S. *Chem. Rev.* **2006**, *106*, 3652.
105. Rowan, S.J.; Cantrill, S.J.; Cousins, G.R.L.; Sanders, J.K.M.; Stoddart, J.F. *Angew. Chem. Int. Ed. Engl.* **2002**, *41*, 898.
106. Lehn, J.-M. *Chem. Eur. J.* **1999**, *5*, 2455.
107. Goral, V.; Nelen, M.I.; Eliseev, A.V.; Lehn, J.M. *Proc. Natl. Acad. Sci. U.S.A.* **2001**, *98*, 1347.

-
108. Brisig, B.; Constable, E.C.; Housecroft, C.E. *New J. Chem.* **2007**, *31*, 1437.
 109. Warren, R.M.L.; Lappin, A.G.; Dev Mehta, B.; Neumann, H.M. *Inorg. Chem.* **1990**, *29*, 4185.
 110. Beattie, J.K.; Elsbernd, H. *Inorg. Chim. Acta* **1995**, *240*, 641.
 111. Chow, H.S.; Constable, E.C.; Housecroft, C.E.; Kulicke, K.; Tao, Y. *Dalton Trans.* **2005**, 236.
 112. Fraenkel-Conrat, H.; Williams, R.C. *Proc. Natl. Acad. Sci. U.S.A.* **1955**, *41*, 690.
 113. Sun, Q.-F.; Iwasa, J.; Ogawa, D.; Ishido, Y.; Sato, S.; Ozeki, T.; Sei, Y.; Yamaguchi, K.; Fujita, M. *Science* **2010**, *328*, 1144.
 114. Chichak, K.S.; Cantrill, S.J.; Pease, A.R.; Chiu, S.-H.; Cave, G.W.V.; Atwood, J.L.; Stoddart, J.F. *Science* **2004**, *304*, 1308.
 115. Steed, J.W.; Atwood, J.L. *Supramolecular Chemistry*, 2nd Edition; Wiley: Weinheim, 2009.
 116. Ariga, K.; Kunitake, T. *Supramolecular Chemistry - Fundamentals and Applications*; Springer: Berlin, 2006.
 117. Lehn, J.-M. *Supramolecular Chemistry: Concepts and Perspectives*; Wiley: Weinheim, 1995.
 118. Dodziuk, H. *Introduction to Supramolecular Chemistry*; Springer: Berlin, 2007.
 119. Steed, J.W.; Turner, D.R.; Wallace, K. *Core Concepts in Supramolecular Chemistry and Nanochemistry*; Wiley: Weinheim, 2007.
 120. Clegg, P.J. *Supramolecular Chemistry: From Biological Inspiration to Biomedical Applications*; Springer: Berlin, 2010.
 121. Hunter, C.A.; Sanders, J.K.M. *J. Am. Chem. Soc.* **1990**, *112*, 5525.
 122. Martinez, C.R.; Iverson, B.L. *Chem. Sci.* **2012**, *3*, 2191.
 123. Chang, H.; Bard, A.J. *Langmuir* **1991**, *7*, 1143.
 124. Kinoshita, K. *Carbon: Electrochemical and physical properties*; Wiley: New York, 1988.
 125. Moore, A.W. In *Chemistry and Physics of Carbon*; Walker, P. L., Jr., Thrower, P. A., Eds.; Marcel Dekker: New York, 1973; Vol. 11, pp 69-187.
 126. Moore, A.W. *Chemistry and Physics of Carbon*; Walker, P. L., Jr., Thrower, P. A., Eds.; Marcel Dekker: New York, 1981; Vol. 17, pp 233-286.
 127. Strosio, J.A.; Kaiser, W.J. *Scanning Tunneling Microscopy*; Academic Press: New York, 2013.
 128. Hermann, B.A.; Scherer, L.J.; Housecroft, C.E.; Constable, E.C. *Adv. Funct. Mater.* **2006**, *16*, 221.
 129. Fréchet, J. *Proc. Natl. Acad. Sci.* **2002**, *99*, 4782.
 130. Tomalia, D.A.; Fréchet, J.M.J. *J. Polym. Sci. A Polym. Chem.* **2002**, *40*, 2719.
 131. Constable, E.C.; Hermann, B.A.; Housecroft, C.E.; Merz, L.; Scherer, L.J. *Chem. Commun.* **2004**, 928.
 132. Scherer, L.J.; Merz, L.; Constable, E.C.; Housecroft, C.E.; Neuburger, M.; Hermann, B.A. *J. Am. Chem. Soc.* **2005**, *127*, 4033.
 133. Scherer, L.J. Ph.D. Thesis, University of Basel, 2006.
 134. Merz, L.; Güntherodt, H.-J.; Hermann, B.A.; Scherer, L.J.; Housecroft, C.E.; Constable, E.C. *Chem. – Eur. J.* **2005**, *11*, 2307.
 135. Constable, E.C.; Hermann, B.A.; Housecroft, C.E.; Neuburger, M.; Schaffner, S.; L. Scherer *New J. Chem.* **2005**, *29*, 1475.

-
136. Constable, E.C.; Häusler, M.; Hermann, B.A.; Housecroft, C.E.; Neuburger, M.; Schaffner, S.; Scherer, L.J. *CrystEngComm* **2007**, *9*, 176.
137. Constable, E.C.; Graber, S.; Hermann, B.A.; Housecroft, C.E.; Malarek, M.S.; Scherer, L.J. *Eur. J. Org. Chem.* **2008**, 2644.
138. Rohr, C.; Gamba, M.B.; Gruber, K.; Constable, E.; Frey, E.; Franosch, T.; Hermann, B.A. *Nano Lett.* **2010**, *10*, 833.
139. Gruber, K.; Rohr, C.; Scherer, L.J.; Malarek, M.S.; Constable, E.C.; Hermann, B.A. *Adv. Mater.* **2011**, *23*, 2195.
140. Rohr, C.; Balbás Gamba, M.; Gruber, K.; Höhl, C.; Malarek, M.S.; Scherer, L.J.; Constable, E.C.; Franosch, T.; Hermann, B.A. *Chem. Commun.* **2011**, *47*, 1800.
141. Figgemeier, E.; Merz, L.; Hermann, B.A.; Zimmermann, Y.C.; Housecroft, C.E.; Güntherodt, H.-J.; Constable, E.C. *J. Phys. Chem. B.* **2003**, *107*, 1157.
142. Zimmermann, Y.C. Ph.D. Thesis, University of Basel, 2002.
143. Nazeeruddin, Md.K.; Baranoff, E.; Graetzel, M. *Solar Energy* **2011**, *85*, 1172.
144. Grätzel, M. *Acc. Chem. Res.* **2009**, *42*, 1788.
145. Grätzel, M. *Inorg. Chem.* **2005**, *44*, 6841.
146. Hagfeldt, A.; Boschloo, G.; Sun, L.; Kloo, L.; Pettersson, H. *Chem. Rev.* **2010**, *110*, 6595.
147. Bora, D.K.; Müller, U.; Constable, E.C.; Braun, A. *J. Electrochem. Soc.* **2017**, *164*, H526.
148. Bora, D.K.; Braun, A.; Erni, R.; Müller, U.; Doebeli, M.; Constable, E.C. *Phys. Chem. Chem. Phys.* **2013**, *15*, 12648
149. Gajda-Schranz, K.; Tymen, S.; Boudoire, F.; Toth, R.; Bora, D.K.; Calvet, W.; Graetzel, M.; Constable, E.C.; Braun, A. *Phys. Chem. Chem. Phys.* **2013**, *15*, 1443
150. Bora, D.K.; Hu, Y.; Thiess, S.; Erat, S.; Feng, X.; Mukherjee, S.; Fortunato, G.; Gaillard, N.; Toth, R.; Gajda-Schranz, K.; Drube, W.; Graetzel, M.; Guo, J.; Zhu, J.; Constable, E.C.; Sarma, D.D.; Wang, H.; Braun, A. *J. Electron Spectrosc. Relat. Phenom.* **2013**, *190*, 93.
151. Bora, D.K.; Braun, A.; Erat, S.; Ariffin, A.K.; Lohnert, R.; Sivula, K.; Topfer, J.; Graetzel, M.; Manzke, R.; Graule, T.; Constable, E.C. *J. Phys. Chem. C* **2011**, *115*, 5619.
152. Bora, D.K.; Braun, A.; S. Erat, S.; Safonova, O.; Graule, T.; Constable, E.C. *arXiv.org, e-Print Arch., Condens. Matter* **2011**, 1-27, arXiv:1111.6204v1.
153. Bora, D.K.; Braun, A.; Erni, R.; Fortunato, G.; Graule, T.; Constable, E.C. *Chem. Mater.* **2011**, *23*, 2051.
154. Braun, A.; Sivula, K.; Bora, D.K.; Zhu, J.; Zhang, L.; Graetzel, M.; Guo, J.; Constable, E.C. *J. Phys. Chem. C* **2012**, *116*, 16870.
155. Bora, D.K.; Rozhkova, E.A.; Schranz, K.; Wyss, P.P.; Braun, A.; Graule, T.; Constable, E.C. *Adv. Funct. Mater.* **2012**, *22*, 490.
156. Hu, Y.; Bora, D.K.; Boudoire, F.; Haussler, F.; Graetzel, M.; Constable, E.C.; Braun, A. *J. Renewable Sustainable Energy* **2013**, *5*, 043109/1.
157. Bozic-Weber, B.; Constable, E.C.; Housecroft, C.E. *Coord. Chem. Rev.* **2013**, *257*, 3089.
158. Housecroft, C.E.; Constable, E.C. *Chem. Soc. Rev.* **2015**, *44*, 8386.
159. Armaroli, N. *Chem. Soc. Rev.* **2001**, *30*, 113.
160. Armaroli, N.; Accorsi, G.; Cardinali, F.; Listorti, A. *Top. Curr. Chem.* **2007**, *280*, 69 and references therein

-
- 161 Boudebous, A.; Constable, E.C.; Housecroft, C.E.; Neuburger, M.; Schaffner, S.; Listorti, A.; Sabatini, C.; Barigelletti, F. *Inorg. Chim. Acta*, **2009**, *362*, 1825.
162. Alonse-Vante, N.; Nierengarten, J.-F.; Sauvage, J.-P. *J. Chem. Soc., Dalton Trans.* **1996**, 1649.
163. Sakaki, S.; Kuroki, T.; Hamada, T. *J. Chem. Soc., Dalton Trans.* **2002**, 840.
164. Bessho, T.; Constable, E.C.; Graetzel, M.; Hernandez Redondo, A.; Housecroft, C.E.; Kylberg, W.; Nazeeruddin, Md. K.; Neuburger, M.; Schaffner, S. *Chem. Commun.* **2008**, 3717.
- 165 Constable, E.C.; Hernandez Redondo, A.; Housecroft, C.E, Neuburger, M.; Schaffner, S. *Dalton Trans.* **2009**, 6634.
- 166 Hernandez Redondo, A.; Constable, E.C.; Housecroft, C.E. *Chimia* **2009**, *63*, 205.
- 167 Sandroni, M.; Pellegrin, Y.; Odobel, F. *C. R. Chimie* **2016**, *19*, 79.
- 168 Fraser, M.G.; van der Salm, H.; Cameron, S.A.; Blackman, A.G.; Gordon, K.C. *Inorg. Chem.* **2013**, *52*, 2980.
- 169 Sandroni, M.; Favereau, L.; Planchat, A.; Akdas-Kilig, H.; Szuwarski, N.; Pellegrin, Y.; Blart, E.; Le Bozec, H.; Boujtita, M.; Odobel, F. *J. Mater. Chem. A* **2014**, *2*, 9944.
- 170 Sandroni, M.; Kayanuma, M.; Rebarz, M.; Akdas-Kilig, H.; Pellegrin, Y.; Blart, E.; Le Bozec, H.; Daniel, C.; Odobel, F. *Dalton Trans.* **2013**, *42*, 14628.
- 171 Kohler, L.; Hayes, D.; Hong, J.Y.; Carter, T.J.; Shelby, M.L.; Fransted, K.A.; Chen, L.X.; Mulfort, K.L. *Dalton Trans.* **2016**, *45*, 9871.
- 172 Sandroni, M.; Kayanuma, M.; Planchat, A.; Szuwarski, N.; Blart, E.; Pellegrin, Y.; Daniel, C.; Boujtita, M.; Odobel, F. *Dalton Transactions*, **2013**, *42*, 10818.
- 173 Martin, C.J.; Bozic-Weber, B.; Constable, E.C.; Glatzel, T.; Housecroft, C.E.; Wright, I.A. *Electrochim. Acta* **2014**, *119*, 86
- 174 Martin, C.J.; Bozic-Weber, B.; Constable, E.C.; Glatzel, T.; Housecroft, C.E.; Wright, I.A. *J. Phys. Chem. C* **2014**, *118*, 16912.
- 175 Fürer, S.O.; Luu, L.Y.N.; Bozic-Weber, B.; Constable, E.C.; Housecroft, C.E. *Dyes Pigm.* **2016**, *132*, 72
- 176 Bozic-Weber, B.; Constable, E.C.; Fürer, S.O.; Housecroft, C.E.; Troxler, L.J.; Zampese, J.A. *Chem. Commun.* **2013**, *49*, 7222.
- 177 Fürer, S.O.; Bozic-Weber, B.; Schefer, T.; Wobill, C.; Constable, E.C.; Housecroft, C.E.; Willgert M. *J. Mater. Chem. A* **2016**, *4*, 12995
178. Balzani, V.; Campagna, S.; Denti, G.; Juris, A.; Serroni, S.; Venturi, M. *Acc. Chem. Res.* **1988**, *31*, 26.
- 179 Constable, E.C. *Coordination Chemistry of Macrocyclic Compounds*; OUP: Oxford, 1999.
- 180 Lindoy, L.F.; Atkinson, I.M.; *Self-Assembly in Supramolecular Systems*; Royal Society of Chemistry: Cambridge UK, 2000.
- 181 Schönhofer, E.; Bozic-Weber, B.; Martin, C.J.; Constable, E.C.; Housecroft, C.E.; Zampese, J.A. *Dyes Pigm.* **2015**, *115*, 154
- 182 Bozic-Weber, B.; Chaurin, V.; Constable, E.C.; Housecroft, C.E.; Meuwly, M.; Neuburger, M.; Rudd, J.A.; Schönhofer, E.; Siegfried, L. *Dalton Trans.* **2012**, *41*, 14157.
- 183 Bozic-Weber, B.; Brauchli, S.Y.; Constable, E.C.; Fürer, S.O.; Housecroft, C.E.; Wright, I.A. *Phys. Chem. Chem. Phys.* **2013**, *15*, 4500.

-
- 184 Henning, A.; Gunzburger, G.; Johr, R.; Rosenwaks, Y.; Bozic-Weber, B.; Housecroft, C.E.; Constable, E.C.; Meyer, E.; Glatzel, T. *Beilstein J. Nanotechnol.* **2013**, *4*, 418.
- 185 Bozic-Weber, B.; Brauchli, S.Y.; Constable, E.C.; Furer, S.O.; Housecroft, C.E.; Malzner, F.J.; Wright, I.A.; Zampese, J.A. *Dalton Trans.* **2013**, *42*, 12293.
- 186 Brauchli, S.Y.; Bozic-Weber, B.; Constable, E.C.; Hostettler, N.; Housecroft, C.E.; Zampese, J.A. *RSC Adv.* **2014**, *4*, 34801.
- 187 Malzner, F.J.; Brauchli, S.Y.; Constable, E.C.; Housecroft, C.E.; Neuburger, M. *RSC Adv.* **2014**, *4*, 48712.
- 188 Brauchli, S.Y.; Malzner, F.J.; Constable, E.C.; Housecroft, C.E. *RSC Adv.* **2014**, *4*, 62728.
- 189 Malzner, F.J.; Willgert, M.; Constable, E.C.; Housecroft, C.E. *J. Mater. Chem. A* **2017**, *5*, 13717
- 190 Malzner, F.J.; Prescimone, A.; Constable, E.C.; Housecroft, C.E.; Willgert, M. *J. Mater. Chem. A* **2017**, *5*, 4671.
- 191 Klein, Y.M.; Willgert, M.; Prescimone, A.; Constable, E.C.; Housecroft, C.E. *Dalton Trans.* **2016**, *45*, 4659
- 192 Baumgartner, Y.; Klein, Y.M.; Constable, E.C.; Housecroft, C.E.; Willgert, M. *RSC Adv.* **2016**, *6*, 86220
- 193 Buttner, A.; Brauchli, S.Y.; Vogt, R.; Constable, E.C.; Housecroft, C.E. *RSC Adv.* **2016**, *6*, 5205.
- 194 Brunner, F.; Klein, Y.M.; Keller, S.; Morris, C.D.; Prescimone, A.; Constable, E.C.; Housecroft, C.E. *RSC Adv.* **2015**, *5*, 58694.
- 195 Brauchli, S.Y.; Constable, E.C.; Housecroft, C.E. *Dyes Pigm.* **2015**, *113*, 447.
- 196 Furer, S.O.; Bozic-Weber, B.; Neuburger, M.; Constable, E.C.; Housecroft, C.E. *RSC Adv.* **2015**, *5*, 69430.
- 197 Willgert, M.; Boujemaoui, A.; Malmstrom, E.; Constable, E.C.; Housecroft, C.E. *RSC Adv.* **2016**, *6*, 56571.
- 198 Brauchli, S.Y.; Malzner, F.J.; Constable, E.C.; Housecroft, C.E. *RSC Adv.* **2015**, *5*, 48516.
- 199 Bozic-Weber, B.; Constable, E.C.; Hostettler, N.; Housecroft, C.E.; Schmitt, R.; Schönhofer, E. *Chem. Commun.* **2012**, *48*, 5727.
- 200 Hostettler, N.; Wright, I.A.; Bozic-Weber, B.; Constable, E.C.; Housecroft, C.E. *RSC Adv.* **2015**, *5*, 37906.
- 201 Hostettler, N.; Furer, S.O.; Bozic-Weber, B.; Constable, E.C.; Housecroft, C.E. *Dyes Pigm.* **2015**, *116*, 124.